# OXYGEN ISOTOPE THERMOMETRY IN CONTACT METAMORPHOSED BIWABIK IRON-FORMATION

by

Elizabeth Priest Valaas

A thesis submitted in partial fulfillment of the
requirements for the degree of

MASTER OF SCIENCE
(Geology)

at the
UNIVERSITY OF WISCONSIN
2004

TABLE OF CONTENTS

ACKNOWLEDGEMENTS

I would like to thank John Valley, my advisor, for all of his encouragement and guidance. Thanks to Clark Johnson for input and critiques. Thanks are also due to Mike Spicuzza for lab training, technical advice, repairs that kept my research going; as well as his patience for all my questions, large and small. Brian Hess is thanked for making both thin and thick sections, which greatly facilitated work on the finer grained samples.

Financial support for my field work was provided by a grant from the Geological Society of America and a Grant-in-Aid of Research from Sigma Xi. My salary and lab expenses were funded by a grant from the National Science Foundation, NSF EAR 02 07340.

Thank you to my cohorts. I appreciate all the time they took to explain, listen, read, and critique. Finally, thank you to my family and friends who supported me throughout.

**ABSTRACT**

The Biwabik, a 1.9 Ga banded iron-formation (BIF) of northern Minnesota, underwent contact metamorphism by the intrusion of the Duluth Complex in the Late Precambrian, 1.1 Ga. The Duluth Complex contact is sub-parallel, but intersects the Biwabik iron-formation. The eastern 25 km of the Biwabik iron-formation is well exposed with nearly continuous outcrops in mines, is contact metamorphosed, and has sub-equal proportions of quartz and magnetite, making it ideal for a quartz-magnetite thermometry study.

Oxygen isotope thermometry has been conducted on coexisting quartz and magnetite in the Biwabik iron-formation. Quartz-magnetite pairs were separated from 63 samples collected at distances of 0-25 km from the eastern end of the formation. Outcrop tests to evaluate variation of $\Delta^{18}O$ (Qt-Mt) within domains measuring 2-10 m were performed by collecting multiple rocks for analysis from each outcrop.

Temperatures, calculated from the $\Delta^{18}O$ (Qt-Mt) thermometer (Clayton and Kieffer, 1991), decrease from 700°C at the contact to 375°C at greater than 2.6 km (measured in three dimensions normal to the contact) based on a second order polynomial curve fit through the data. The temperatures of this study are ~70°C higher at the contact than those of Perry and Bonnichsen (1966). The temperatures at the grunerite and fayalite isograds were used to estimate the depth at which the Duluth Complex was emplaced. The pressure estimated is 0.6 ±0.2 kb and depth 2.2 ±1.5 km based on reaction of grunerite = fayalite + quartz + $H_2O$ and consistent with minnesotaite = grunerite + quartz + $H_2O$ (Evans and Guggenheim, 1988; Jenkins and Bozhilov, 2003).

The $\Delta^{18}O$ (Qt-Mt) temperatures and $\delta^{18}O$ (Qt) values were used to estimate depositional $\delta^{18}O$ values of quartz, and the water from which the BIF minerals, or precursors, precipitated at 1.9 Ga. Interpretation of these values involve examining three hypotheses: 1) the calculated quartz values are correct and ocean water had a lower $\delta^{18}O$ value in the Precambrian, 2) hotter ocean temperatures could explain the measured quartz values and $\delta^{18}O$ water has remained at ~0‰ since 1.9 Ga, and 3) resetting of the values through alteration. The resetting of the values during diagenesis or metamorphism is concluded, preventing estimates of temperature and composition of the ocean at 1.9 Ga.

## INTRODUCTION

This study presents the results of $\Delta^{18}O$ (Qt-Mt) thermometry of the 1.9 Ga Biwabik banded iron-formation (BIF) in northern Minnesota. Quartz-magnetite is a good thermometer because the fractionation is large and temperature sensitive relative to other mineral pairs and the effects of crystal chemistry and solid solution are small (Valley, 2001). This study revisits thermometry by Perry and Bonnichsen (1966) using newer techniques that allow accurate measurement of $\delta^{18}O$ from samples ~10 times smaller, which is important in fine grained rocks like the Biwabik iron-formation.

The oxygen isotope composition of Precambrian seawater is controversial. The data of the study are used to estimate the depositional $\delta^{18}O$ values of the quartz, and $\delta^{18}O$ of the water from which the quartz, or the opaline ooze precursor, precipitated. Precambrian $\delta^{18}O$ (Qt) values are lower than values in the Phanerozoic (Perry et al., 1973; Becker and Clayton, 1976; Robert et al., 1992; Winter and Knauth, 1992; Knauth and Lowe, 2003; Perry and Lefticariu, 2003). To understand Precambrian sea water $\delta^{18}O$ and implications on ocean temperature, three hypotheses have been proposed: 1) measured $\delta^{18}O$ (Qt) from BIFs have not been reset and the sea water had lower $\delta^{18}O$ values in the Precambrian, 2) measured $\delta^{18}O$ (Qt) values have not been reset and sea water has remained at ~0‰ since the Precambrian, and hotter sea water temperatures produced the lower Precambrian $\delta^{18}O$ (Qt) values, and 3) $\delta^{18}O$ (Qt) values have been reset through alteration.

All samples referenced in this thesis are in the collections of the Department of Geology and Geophysics Museum, University of Wisconsin, Madison, under file number UW 1962.

## REGIONAL GEOLOGY

The 1.9 Ga Biwabik iron-formation trends east-northeast for 190 km across northern Minnesota and is cut by the Duluth Complex at its eastern end near Babbitt, Minnesota (Perry and Bonnichsen, 1966; Morey, 1972). The iron-formation was deposited with quartzite and black shale in a continental shelf environment (Gundersen and Schwartz, 1962; Morey, 1983) and is classified as a Superior-type BIF (Gross, 1979). The Biwabik iron-formation was deposited in the Animikie Basin which covered northern and east-central Minnesota, southeastern Ontario, northern Michigan and northern Wisconsin. The Biwabik iron-formation produces ore that is 25-30% iron and has been mined since 1892 (Morey, 1972). The Virginia formation overlies, and Lower Precambrian rocks (Fig. 1) and locally the Pokegama quartzite underlie the iron-formation. The sedimentary bedding dips 45-30° southward at the northeastern end closest to the contact with the Duluth Complex and the shallows to 5° within a few km along strike. The contact of Duluth Complex with the country rock dips 20-30° along the northwestern edge and systematically increases to as much as 60° SE (Fig. 1).

The Biwabik iron-formation ranges in thickness from less than 60 m to about 215 m (Bonnichsen, 1975; Morey, 1983). It thins to the east where it is intruded by the Duluth Complex. Stratigraphically the iron-formation is divided into four main units: the Lower Cherty, Lower Slaty, Upper Cherty, and Upper Slaty (Gundersen, and Schwartz, 1962; Bonnichsen, 1975). The cherty layers are massive, quartz-rich, richer in magnetite, and have a more granular texture that suggests the layers were deposited in a shallow water, high energy environment. In contrast, the slaty layers are fine grained, laminated, rich in iron silicates and carbonates, and were deposited in a deeper water, low energy environment. The

repetition of the different depositional environments (Morey, 1972) suggests fluctuation of the relative location of the strand line reflecting the deepening of the Animikie Basin followed by infilling.

The emplacement of the Duluth Complex, 1106-1096 Ma (Hauk et al., 1997), resulted in contact metamorphism of the Biwabik iron-formation. The Duluth Complex in northern Minnesota is related to the mid-continent rift that extends from Ohio to Minnesota and south to Kansas (Weiblen and Morey, 1980; Hauk et al., 1997). The Duluth Complex is composed of a variety of rock types, which include troctolitic, gabbroic, anorthositic, granodioritic and granitic bodies. The Biwabik iron-formation was intruded by the troctolitic South Kawishiwi and Partridge River intrusions (Weiblen and Morey, 1980; Hauk et al., 1997). The emplacement temperature of the Duluth Complex was ~1150 °C (Koptev-Dornikov et al., 1995), causing pyroxene hornfels facies metamorphism in the Biwabik iron-formation nearest to the contact (Hauk et al., 1997).

Isograds have been mapped in the Biwabik iron-formation sub-parallel to the present day contact with the Duluth Complex (French, 1968). The isograds shown in Fig. 2 are: 1) the partial reduction of hematite to magnetite, 2) the formation of clinozoisite, 3) the formation of grunerite, 4) the formation of hedenbergite and the complete reduction of hematite to magnetite, and 5) the formation of ferrohypersthene along with the development of crystalline graphite. These isograds have been refined and expanded by Frost (2001) to include 6) the formation of hedenbergite, 7) the formation of fayalite, and 8) the formation of orthopyroxene.

## METHODS

The oxygen isotopic ratios of coexisting quartz and magnetite were measured for samples from the Biwabik iron-formation from the eastern-most ~25 km which was contact metamorphosed by the Duluth Complex. Sampling localities are shown in Fig. 2. Distances to the contact (Table 1) are 3-D distances unless noted as map distances. No samples were collected from 350-2500 m (map) to the contact due to active mining and mine flooding. Each sample is identified by the numbering system: 03 BIW XY-Z, where X = outcrop number, Y = letter to differentiate hand samples, Z = number that differentiates areas of interest in a hand sample (if necessary) (Table 1). Samples followed by M1, 2, or 3 indicate multiple magnetite areas in a thick microscope slide analyzed along and off strike of the original magnetite analyzed (Table 1).

The 3-D distances have been corrected from map distance using the dip of the contact to estimate the distance perpendicular to the projected base of the Duluth Complex. The correction is based on measured dips of the base of the Duluth Complex (Bonnichsen, 1972), which vary from 20-30° in the northern part of the study area and increase to 60° farther south (Fig. 1). For simplification, 30° was assumed for the northern part, and 60° for samples in the southwestern part of the study area. The isograds of French (1968) are closer together where the dip of the contact is steeper and farther apart where the dip of the contact is shallower (Figs. 1 & 2), this suggests that the dip of the contact directly over the samples may have been variable and supports the distance corrections of this study.

It was possible to hand pick quartz and magnetite from coarse samples, those yielding mineral grains of ~300-1000 μm diameter, located closer to the contact. Pieces were taken from a "thick section," a rectangular slice of the hand sample that has standard thin section

dimensions but is 800-1000 μm thick. The locations of the areas sampled in each thick section were digitally recorded on scanned images in Adobe Illustrator. The pieces were crushed and sieved. Grains greater than 150 μm were separated by hand magnet to concentrate the magnetite from the quartz and other silicates. Once the magnetite was separated, the remainder was soaked in 12.4 M hydrochloric acid to remove any residual magnetite. After rinsing and drying, the mineral separate was hand picked for quartz. The concentrate of magnetite was not acid treated, but picked directly. Composite grains were avoided, although that was more difficult to evaluate for coarser magnetite grains, ~600-1000 μm. Euhedral magnetite grains were chosen to ensure no contamination by adhered silicates.

For samples from greater than 100 m from the contact, quartz was difficult but possible to hand pick, but magnetite was not. These thick sections were cut with a thin diamond saw blade to sample magnetite. Parallel cuts along magnetite-rich layers made strips ~ 0.8 x 1 x 20 mm; the dimensions depended on the thickness and width of the magnetite layer of interest. Sawing also gave precise location of the analysis sample within the thick section. Pieces weighing approximately 2 mg (~0.5 $mm^3$) were selected from the strips of magnetite-rich layers for analysis. Adjacent material, on strike, was set aside for purity tests. The amount of silicate impurities in these magnetite samples was estimated by measuring the mass of the adjacent piece before dissolution of magnetite by HCl and again afterwards once rinsed and dried. The samples that were greater than 20% non-magnetite by mass were rejected for analysis. For samples greater than 3 km from the contact, magnetite was found to be the most pure (less than 20 % non-magnetite by mass) in oval nonoölitic granules ~4 x 10 mm, rather than in the layers. The magnetite-rich layers at greater than 3 km from the

contact had silicates interspersed and were greater than 20% non-magnetite by mass. The granule magnetite was analyzed.

Oxygen was extracted from 0.5-1.5 mg of quartz and 1.75-2.75 mg of magnetite by $CO_2$ laser heating and fluorination with $BrF_5$ as the reagent (Spicuzza et al., 1998). The liberated oxygen was converted to $CO_2$ for analysis using a Finnigan MAT 251 mass spectrometer. The oxygen isotope ratios are shown in standard per mil format, relative to V-SMOW. Five analyses of NBS-28 (quartz) yielded $\delta^{18}O = 9.41 \pm 0.20‰$. The standard, UWG-2 (Gore Mountain garnet), was run ~ 6 times on each day of analysis. 114 analyses of UWG-2 for $\delta^{18}O$ yielded a mean daily standard deviation of ±0.08‰. The UWG-2 $\delta^{18}O$ was standardized to 5.8‰ (Valley et al., 1995) for accuracy; the average correction was 0.11‰ (absolute value). Samples were corrected by the same amount as UWG-2 for each day of analysis.

To correct the sawed magnetite pieces, the $\delta^{18}O$ contamination was estimated from the silicate residue after dissolution in HCl. These minerals, as identified in thin sections, included quartz, greenalite, minnesotaite, and stilpnomelane in low grade rocks; and quartz, grunerite, hedenbergite, and fayalite in higher grade ones. The percentages of quartz and other silicates were estimated from grain mounts of the residue in refractive oil (RI = 1.558) using a petrographic microscope. Corrections were made assuming the residue quartz had no inclusions. The other silicates were approximated as diopside. The residue silicate percentages were converted into fractions of $\delta^{18}O$ values of quartz and diopside to subtract from the measured $\delta^{18}O$ (Mt) (Table 2). Quartz contamination was based on measured $\delta^{18}O$ (Qt). Minerals other than quartz were given $\delta^{18}O$ diopside values calculated from $\Delta^{18}O$ (Qt-Di) (Table 2; Clayton and Kieffer, 1991):

$$1000 \ln\alpha \text{ (Qt-Di)} = (2.75*10^6)/(T)^2 \approx \Delta^{18}O \text{ (Qt-Di)} \qquad T \text{ in } °K \qquad \textbf{(1)}$$

using the measured $\delta^{18}O$ (Qt) and temperature from the $\Delta^{18}O$ (Qt-Mt) thermometer (Clayton and Kieffer, 1991):

$$1000 \ln\alpha \text{ (Qt-Mt)} = (6.29*10^6)/(T)^2 \approx \Delta^{18}O \text{ (Qt-Mt)} \qquad T \text{ in } °K \qquad \textbf{(2)}$$

using the $\Delta^{18}O$ (Qt-Mt) value calculated with the uncorrected $\delta^{18}O$ (Mt) value, as an approximation.

Metamorphic temperatures of the Biwabik iron-formation were calculated by equation (2) using corrected $\delta^{18}O$ (Mt) values. A curve was fit through the data using a second order polynomial. Temperatures for this study are based on this curve unless otherwise noted by a specific outcrop. Using this curve fit averages out variability in the data.

Whole rock $\delta^{18}O$ values were calculated to evaluate whether the Biwabik iron-formation experienced a closed or open system with respect to fluids. To calculate $\delta^{18}O$ (whole rock), the amounts of quartz and magnetite were estimated. The relative modal amounts of quartz and magnetite were calculated using thin sections, a digital Photoshop image, and the NIH Image program (http://rsb.info.nih.gov/nih-image/). These proportions were scaled to 1000 ml. Minerals other than magnetite were estimated as quartz. The quartz and magnetite volumes were divided by their respective molar volumes to get moles/1000 ml. The result for magnetite was multiplied by two because the mineral has twice as many oxygen atoms per formula unit as quartz. Then, the analyzed $\delta^{18}O$ (Qt) and $\delta^{18}O$ (Mt) were multiplied by their respective molar oxygen fraction, and added together, to estimate a whole rock (WR) value (Table 3):

$$\delta^{18}O \text{ WR} = [\text{O mole fraction (Qt)}*\delta^{18}O \text{ (Qt)}] + [\text{O mol fraction (Mt)}*\delta^{18}O \text{ (Mt)}] \qquad \textbf{(3)}$$

Depositional values for quartz were estimated by equation (3) and $\Delta^{18}O$ (Qt-Mt). Extrapolating equation (2) to such low temperatures is not valid since calibration experiments were conducted at temperatures equal to and greater than 600°C and extrapolation is recommended for above ~125°C only (Clayton and Kieffer, 1991). Instead, a $\Delta^{18}O$ (Qt-Mt) calibration for low temperature was calculated from the $\Delta^{18}O$ (silica-water) calibration of Brandriss et al. (1998):

$$1000 \ln\alpha \text{ (silica-water)} = (15.56*10^3/T) - 20.92 \approx \Delta^{18}O \text{ (silica-water)} \quad T \text{ in } °K \qquad \textbf{(4)}$$

and $\Delta^{18}O$ (Mt-water) calibration of Mandernak et al. (1999):

$$1000 \ln\alpha \text{ (Mt-water)} = 0.79*10^6/(T)^2 - 7.64 \approx \Delta^{18}O \text{ (Mt-water)} \quad T \text{ in } °K \qquad \textbf{(5)}$$

The calculated $\Delta^{18}O$ (Qt-Mt) from equations 4 & 5 is:

$$1000 \ln \alpha \text{ (Qt-Mt)} = 2.3*10^6/(273+T)^2 + 4.35 \approx \Delta^{18}O \text{ (Qt-Mt)} \quad T \text{ in } °K \qquad \textbf{(6)}$$

Equation (6) ignores affects due to salt or hydrous components in silica. Equations (3) and (6) were solved simultaneously for the $\delta^{18}O$ of depositional quartz at 55°C, an estimate of the ocean water temperature from which the quartz and magnetite precipitated based on sea water temperatures for the Precambrian (Knauth, 1998; Winhusen, 2000). The calculated $\delta^{18}O$ (Qt) was then used in equation (4) to estimate the $\delta^{18}O$ of sea water at the time of the deposition of the Biwabik iron-formation. The calculations were repeated for 45°C and 65°C to evaluate the effect of temperature on the $\delta^{18}O$ estimate for ocean water.

## ROCK AND SAMPLE DESCRIPTIONS

The BIF samples from nearest to the contact with the Duluth Complex are the coarsest grained due to recrystallization during metamorphism, with a gradational shift to finer grained rocks that preserve sedimentary features at distances greater than 3 km from the

contact. All samples are from the Upper Cherty unit of the Biwabik iron-formation. This unit was chosen for its magnetite, average 26% by mode, since the slaty units are iron silicate-rich and magnetite-poor. The lower cherty unit is less well exposed. Samples were not collected west of the partial reduction of hematite to magnetite isograd ((1); Fig. 2) since magnetite was needed for the study.

Representative samples were examined in thin section to confirm agreement with previously mapped isograds (French, 1968; Frost, 2001). In addition to quartz (chert) + magnetite, the samples furthest from the contact may contain: siderite, ankerite, greenalite, minnesotaite, or stilpnomelane. Minnesotaite forms from two reactions; equation (8) happens to a lesser extent (Bonnichsen, 1975):

greenalite + 2 quartz = minnesotaite + water **(7)**
$(Fe,Mg)_3Si_2O_5(OH)_4 + 2SiO_2 = (Fe,Mg)_3Si_4O_{10}(OH)_2 + H_2O$

3 siderite + 4 quartz + $H_2O$ = minnesotaite + $3CO_2$ **(8)**
$3(Fe,Mg)CO_3 + 4SiO_2 + H_2O = (Fe,Mg)_3Si_4O_{10}(OH)_2 + 3CO_2$

At 2-3 km from the contact, the assemblage is quartz + magnetite + grunerite ± carbonate. Grunerite (isograd 3; Fig. 2) forms during prograde metamorphism only in $H_2O$-rich layers (Bonnichsen, 1975) by this reaction:

7 minnesotaite = 3grunerite + 4 quartz + $4H_2O$ **(9)**
$7(Fe,Mg)_3Si_4O_{10}(OH)_2 = 3(Fe,Mg)_7Si_8O_{22}(OH)_2 + 4SiO_2 + 4H_2O$

Closer to the contact the assemblage shifts to quartz + magnetite ± grunerite ± cummingtonite ± actinolite ± hedenbergite ± fayalite. Orthopyroxene appears closest to the contact. Hedenbergite (isograds 4 & 6; Fig. 2) forms by reaction 10 (French, 1968):

ankerite + 2quartz = hedenbergite + $2CO_2$ **(10)**
$CaFe(CO_3)_2 + 2SiO_2 = CaFeSi_2O_6 + 2CO_2$

Fayalite (isograd 7; Fig. 2) forms by several reactions (French, 1968; Bonnichsen, 1975; Miyano and Klein, 1986):

2 grunerite = 7 fayalite + 9 quartz + $2H_2O$ **(11)**
$2(Fe,Mg)_7Si_8O_{22}(OH)_2 = 7(Fe,Mg)_2SiO_4 + 9SiO_2 + 2H_2O$

2 magnetite + 3 quartz = 3 fayalite + $O_2$ **(12)**
$2Fe_3O_4 + 3SiO_2 = 3(Fe)_2SiO_4 + O_2$

2siderite + quartz = fayalite + $2CO_2$ **(13)**
$2(Fe,Mg)CO_3 + SiO_2 = (Fe,Mg)_2SiO_4 + 2CO_2$

Orthopyroxene (isograd 8; Fig.2) forms by reactions 14 & 15 (Bonnichsen, 1975; Miyano and Klein, 1986):

olivine + quartz = 2 orthopyroxene **(14)**
$(Fe,Mg)_2SiO_4 + SiO_2 = 2(Fe,Mg)SiO_3$

grunerite + siderite = 8 orthopyroxene + $CO_2$ + $H_2O$ **(15)**
$(Fe,Mg)_7Si_8O_{22}(OH)_2 + (Fe,Mg)CO_3 = 8(Fe,Mg)SiO_3 + CO_2 + H_2O$

Fig. 2 shows isograds that reflect the changing mineralogy described above. Garnet, pyrite, and pyrrhotite are locally present in a few higher grade samples. Actinolite, where present, typically rims grunerite or cummingtonite. The actinolite and cummingtonite from nearer the contact were likely formed by retrograde reactions from fayalite and pyroxene (Bonnichsen, 1975).

In samples less than 100 m from the contact, quartz and magnetite occur as coarse grains. The quartz layers are thicker, ~2-10 cm, than the magnetite layers, ~2-8 mm. Samples from 100-3000 m show a gradational shift to finer grained. The quartz layers are ~2-10 cm and the magnetite layers are ~1-5 mm. Quartz and magnetite oölitic and non-oölitic granules locally persist in quartz layers at 100-3000 m. In the samples from greater than 3000 m from

the contact, the rocks sampled are more fine grained and pervasively preserve sedimentary quartz and magnetite oölitic and non-oölitic granules in a quartz (chert) matrix.

## RESULTS

Values of $\delta^{18}O$ were analyzed in quartz and magnetite for 63 samples of the Biwabik iron-formation and $\Delta^{18}O$ (Qt-Mt) was calculated (Table 1). The data used to correct measured values of $\delta^{18}O$ (Mt) for silicate impurities are in Table 2 and whole rock data in Table 3. The oxygen isotope analyses of Perry and Bonnichsen (1966) are presented in Table 4, with temperatures recalculated by equation (2). Sampling localities for this study are shown on a geologic map in Fig. 2, with GPS coordinates in Appendix 2 and a more detailed sample localities map in Appendix 3.

### *Outcrop Tests*

To evaluate the reproducibility of quartz-magnetite fractionation and temperature estimates at the outcrop scale, multiple hand samples were analyzed from several locations. The scale of the outcrops ranges from 2 to10 meters in length. Fractionations from outcrops with three or more hand samples are shown in Fig. 3. The standard deviations of $\Delta^{18}O$ (Qt-Mt) values ranged from ±0.15‰ (±21°C) for outcrop 22 (UW 1962.22) to ±5.35‰ (±82°C) for outcrop 35 (UW 1962.35). The uncertainty was calculated by taking the standard deviation of the average $\Delta^{18}O$ (Qt-Mt) values of the hand samples from each outcrop. The $\Delta^{18}O$ (Qt-Mt) thermometer is less sensitive at higher temperatures. Generally, the variability between hand samples is greater than variability within hand samples. The variability of $\Delta^{18}O$ (Qt-Mt) values increases dramatically outside isograd 3, greater than 2.6 km from the

contact with the Duluth Complex (outcrop 35; Figs. 2 & 3) and are not in equilibrium. The higher grades of metamorphism enable exchange of oxygen isotopes to equilibrate the $\delta^{18}O$ values of the minerals.

There are three ways to calculate precision of the data to assess variability. 1) Analytical uncertainty of individual measurements of $\delta^{18}O$ is based on the reproducibility of garnet standards run on the same day. The garnet had very small average daily precision (±0.08‰; one standard deviation). 2) Precision is also measured for mineral separates from the same thick sections, calculated by the standard deviation of $\delta^{18}O$ (Qt) and $\delta^{18}O$ (Mt) for each thick section (Table 1). Standard deviations for equilibrated samples range from ±0.00 to ±0.32‰ (average = ±0.07‰; one standard deviation) for quartz and ±0.00 to ±0.82‰ (average = 0.10‰; one standard deviation) for magnetite. Outcrop 35 (UW 1962/35) is not equilibrated: although the quartz ranges from ±0.00 to ±0.17‰, the magnetite ranges from ±0.32 to ±1.64‰ (Table 1). 3) The outcrop test measured variation between hand samples in each outcrop, and generally produced the greatest variability (Fig. 3).

To propagate the precision of $\delta^{18}O$ (Qt) and $\delta^{18}O$ (Mt) to $\Delta^{18}O$ (Qt-Mt), the standard deviation for $\Delta^{18}O$ (Qt-Mt) (Table 1) was calculated by:

$$[(\text{std. dev. } \delta^{18}O\ (Qt))^2+(\text{std. dev. } \delta^{18}O\ (Mt))^2]^{1/2} \quad \textbf{(16)}$$

## DISCUSSION

### *Evaluation of isotopic equilibrium*

It is necessary to evaluate whether the measured fractionations represent equilibrium. $\Delta^{18}O$ (Qt-Mt) of outcrops at different distances from the contact are shown in Fig. 3b. The graph shows that for samples less than or equal to 2.6 km from the contact, there is the best

reproducibility of $\Delta^{18}O$ (Qt-Mt) values. The standard deviation of the fractionation values of hand samples from the same outcrop increases sharply outside isograd 3: ±5.35‰ for outcrop 35 (UW 1962/35). The greater variability of $\Delta^{18}O$ (Qt-Mt) outside the grunerite isograd is expected since these values are from the lowest grades of contact metamorphism. Outcrop 36 (UW 1962/36), which is greater than 2.7 km from the contact, has no contact metamorphic silicates as defined by Bonnichsen, (1975). Both outcrops 36 and 35 (UW 1962/36 &35) preserve original sedimentary features: fine grained, oölitic and nonoölitic granules, and fine laminations; suggesting the metamorphism was not hot enough to recrystallize and equilibrate these samples. Although outcrops 35 and 36 agree in temperature: one standard deviation of the temperature of outcrops 35 and 36 overlap (Table 1), they have been excluded from temperature curve determination because quartz and magnetite in these outcrops have not equilibrated. The convergence of the other outcrops suggests that the majority of the Biwabik iron-formation samples have attained and preserved equilibrium at the hand sample (cm) scale.

***Diffusion in magnetite and quartz***

To understand the variability of the $\Delta^{18}O$ (Qt-Mt) values between hand samples, closure temperatures, $T_c$, for diffusion in magnetite and quartz have been calculated by the Dodson (1973) equation:

$$T_c = \frac{(E/R)}{\mathrm{Ln}\left\{ -\frac{A\,R\,T_c^2\,(D_o/a^2)}{E\,(\delta T/\delta t)} \right\}} \qquad \textbf{(17)}$$

Where A = diffusional anisotropy parameter, a = radius of mineral grain (cm), R = gas constant, 8.3143 J/°K*mol, $D_o$ = pre-exponential factor ($cm^2/s$), E = activation energy (J/mol), and $\delta T/\delta t$ = linear cooling rate (°C/s).

Equation (17) was calculated for samples from greater than 2.6 km from the contact, and at the contact with the Duluth Complex. For outcrops 35 & 36 (UW 1962/35 & 36) at greater than 2.6 km from the contact, a grain size of 10 μm in diameter and a cooling rate of 500°C/Ma were used in equation (17) (Table 5). For magnetite at wet conditions ($PH_2O$ = 1 kb), (Giletti and Hess, 1988), the closure temperature is 383°C. The closure temperature for wet quartz ($PH_2O$ = 1 kb; Dennis, 1984) is 286°C, ~100°C lower than magnetite (Table 5). If the only minerals were quartz and magnetite, the $T_c$ of the magnetite would determine the closure temperature of the rock because it has slower diffusion properties than quartz. However, minnesotaite, greenalite, stilpnomelane, and carbonate are present at greater than 10% by mode. After the rock cooled below the magnetite's closure temperature, quartz continued to exchange with these faster diffusion minerals (Fortier and Giletti, 1989; Zheng and Fu, 1998; Valley, 2001) until the quartz reached its $T_c$. This means $T_c$ (Qt) determines the closure temperature of the quartz magnetite pair. The average temperature for outcrops 35 & 36 is 303 ±80°C, slightly above the closure temperature of wet quartz (286°C). The similarity of the temperatures suggests little exchange of oxygen between quartz and magnetite, so the variability of the magnetite may reflect original variation.

The values of $T_c$ were calculated for a grain size of 2 mm in diameter and a cooling rate of 500°C/Ma at the contact with the Duluth Complex. For wet magnetite, $T_c$ is 648°C (Table 5; Giletti and Hess, 1988). $T_c$ for wet quartz at the contact is 561°C, ~90°C lower than magnetite (Table 5; Dennis 1984a). The closure temperatures for both minerals are below the

temperature at the contact: 700°C. Other minerals at the contact are pyroxene, fayalite and minor retrograde amphibole. These minerals have slower diffusion than quartz (Fortier and Giletti, 1989; Zheng and Fu, 1998; Valley, 2001), so the magnetite $T_c$ reflects the closure temperature of the Qt-Mt pair, which requires discussion.

The estimated $\Delta^{18}O$ (Qt-Mt) temperature at the contact is higher than the calculated $T_c$ of wet magnetite, suggesting the inputs for equation (17) (2mm, 500°C/Ma, wet, $PH_2O$ = 1 kb conditions) should be examined. Increasing the grain size in the equation would increase the estimated closure temperature, but 2mm was the largest size analyzed. If the Duluth Complex cooled more quickly, at 2050°C/Ma, the closure temperature of magnetite is equal to the temperature at the contact, 700°C (Table 5). The cooling rate is not unreasonable, suggesting the Duluth Complex cooled quickly.

An alternative hypothesis is that metamorphic conditions at the contact were different. Low water activity at the contact could produce closure temperatures higher than wet conditions. Low water activity is possible by partial melting, by fractures in the rock that reached the surface, or by flow of $CO_2$ at the contact. There have only been reports of partial melting of xenoliths in the Duluth Complex (Ripley and Alawi, 1988; Ripley et al., 2001), not of the Biwabik iron-formation. Also, there does not appear to be evidence of fractures in the petrology of the rocks: the rocks don't appear broken and there is no quartz veining. The slaty members of the iron-formation are richer in graphite (French, 1968), and it is possible that $CO_2$ could have lowered the water activity at the contact.

To see if dry conditions could produce closure temperatures above the temperature calculated from $\Delta^{18}O$ (Qt-Mt) at the contact (Table 5), the quartz closure temperature for dry conditions, 2 mm in diameter, and a dT/dt of 500°C/Ma (Table 5; Sharp et al., 1991) is

787°C (Table 5), ~90°C higher than the curve fit temperature of 700°C at the contact. Dennis (1984b) has a calibration for dry quartz, and the closure temperature is 565°C (Table 5). Assuming the more recent Sharp et al. (1991) calibration is correct, dry quartz $T_c$ above the temperature calculated from $\Delta^{18}O$ (Qt-Mt) is consistent with dry conditions for the Biwabik iron-formation at the contact with the Duluth Complex during contact metamorphism. However, Hauck et al. (1997) hypothesize that devolatilization of the footwall sedimentary rocks, like the Biwabik iron-formation, contributed to syn- to post-magmatic fluids that altered the Duluth Complex rocks and remobilized the sulfide and PGE in the Duluth Complex, which would mean high water activity of the Biwabik iron-formation at the contact.

***Effect of modal proportions of quartz and magnetite on $\delta^{18}O$ (Mt)***

The graph of $\delta^{18}O$ of quartz and magnetite vs. distance (3-D) from the contact (Fig. 4) shows there is more variation in magnetite $\delta^{18}O$ values than quartz $\delta^{18}O$ values. Also plotted in Fig. 4 are the calculated $\delta^{18}O$ (whole rock) values (Table 3). The relatively constant $\delta^{18}O$ (whole rock) values, 12.48 ±0.87‰ for samples less than 0.2 km from the contact and 12.38 ±2.01‰ for samples greater than 2.5 km from the contact, suggest oxygen isotope mass balance in the Biwabik iron-formation. The rocks have a greater proportion of oxygen in quartz than magnetite; the average by mode is 75% quartz and 25% magnetite, so a greater shift in $\delta^{18}O$ (Mt) is expected from mass balance. Fig. 4 also shows how $\delta^{18}O$ of the minerals changes closer to the contact: $\Delta^{18}O$ (Qt-Mt) decreases towards the contact with increasing temperatures.

In Fig. 5, $\delta^{18}O$ (Qt) is plotted against $\delta^{18}O$ (Mt). Isopleths of $\Delta^{18}O$ (Qt-Mt) represent constant equilibrium temperatures of 300, 500, and 900° C (Clayton and Kieffer, 1991). Assuming constant exchange of oxygen between quartz and magnetite with increasing temperatures from the original sediment values, the steep negative slope of the line through the data reflects the modal proportions of quartz and magnetite in the samples. As the rocks were heated and underwent isotopic exchange, quartz represented the larger reservoir of oxygen, so $\delta^{18}O$ (Qt) shifts less than $\delta^{18}O$ (Mt), creating the steep trend to the data (Gregory et al., 1989). Looking at the shape of the data, where there is a positive slope for data near the contact, suggests an alternative hypothesis. There may have been closed system exchange far from the contact, but closer there may have been open system exchange with low $\delta^{18}O$ magmatic water in an inner aureole.

***Temperatures of the Biwabik iron-formation***

Temperatures are plotted against distance from the contact (3-D) (Fig. 6). The temperature closest to the contact is 700°C from the second order polynomial curve fit (Figs. 6a & 6b). One sample is a xenolith in the Duluth Complex which yields 918 ±6°C (Figs. 6a & 6b). Temperature decreases away from the contact to 370°C at 2600 m (Fig. 6a). The uncertainty in the measured temperatures is based one standard deviation of $\Delta^{18}O$ (Qt-Mt) values in equation (2). Outcrops 35 & 36 (UW 1962/35 & 36) produced the lowest temperatures, but the magnetite and quartz are clearly not equilibrated. These outcrops are the lowest in metamorphic grade and lie inside (closer to the contact) only two isograds (Fig. 2, French, 1968). The samples that Perry and Bonnichsen (1966) corrected for true distance

are included. They assumed a constant dip of ~12%, which reduced the horizontal distances by a factor of five (Perry et al., 1973).

Temperatures calculated from $\Delta^{18}O$ (Qt-Mt) values are self-consistent, but differ from previous work. Perry and Bonnichsen's (1966) data yield lower temperatures than this study closest to the contact and higher temperatures than this study at greater than 400 m from the contact (Fig. 6). Additional thermometers provide a check of the $\Delta^{18}O$ (Qt-Mt) thermometry at the contact between the Biwabik iron-formation and the Duluth Complex. The Biwabik iron-formation contains pigeonite and inverted pigeonite close to the contact with the Duluth Complex (Bonnichsen, 1969). The measured pyroxene compositions, which were ~7% $MnSiO_3$, and the orthopyroxene-pigeonite phase boundary, suggest a minimum temperature at the contact of 775°C (Bonnichsen, 1969; Lindsley, 1983). This temperature is 75°C above the contact temperature of the polynomial curve fit to the $\Delta^{18}O$ (Qt-Mt) data and 125°C above the estimate of Perry and Bonnichsen (1966). However, 775°C is within one standard deviation of our estimate at outcrop 40 (UW 1962/40) at the contact: 756 ± 22 °C. Temperatures at the contact of the Duluth Complex and the Virginia formation, as determined by the ubiquitous perthitic nature of K-feldspar and two feldspar geothermometry (Andrews and Ripley, 1987) were 650 °C. This is significantly lower than this study. But feldspars can easily be reset (Bohlen and Essene, 1977).

Simmons et al. (1974) estimated the temperature at the contact of the Duluth Complex and the Gunflint iron-formation at greater than 800 °C from pyroxenes. They assumed that pigeonite crystallized in its stability field (Simmons et al., 1974). Also, the pigeonites were not as rich in Mn as those analyzed by Bonnichsen (1969), increasing the Mn content would lower the Simmons et al. (1974) estimated temperature. The Gunflint iron-

formation is considered to be the continuation of the Biwabik iron-formation ~100 km along strike in Minnesota and Canada. The portion of the Duluth Complex next to the Gunflint may have a different depth and thermal history than next to the Biwabik iron-formation.

In addition, Fe-Ti oxides (Buddington and Lindsley, 1964) and two pyroxene thermometry (Lindsley, 1983), could be used to estimate temperature of metamorphism at the contact. Fe-Ti oxides were reported by Simmons et al. (1974) for the Gunflint iron-formation. While Morey et al. (1972) reported very low titanium content of the Biwabik iron-formation as a whole, it is possible that titanium introduced from the Duluth Complex may yield ilmenite in the iron-formation close to the contact (Simmons et al., 1974). Future electron microprobe analysis to determine mineral compositions would serve to evaluate the alternative thermometers.

***Contact metamorphic thermal profile***

The profile of the $\Delta^{18}O$ (Qt-Mt) temperatures is concave up (Fig. 6), which is predicted for the intrusion and cooling of a simple tabular body. The equation of Jaeger (1957) was used to estimate the contact metamorphic thermal profile. The contact temperature was calculated two ways. Assuming only thermal conduction (Jaeger, 1959):

$$T_{contact} = \sigma T_1/(1 + \sigma) = 668°C \quad \textbf{(18)}$$

Where $T_1$ is $\Delta T$ (melting temperature of the Duluth Complex vs. precontact-metamorphic country rock temperature) = (1150 – 250°C) (French, 1973; Koptev-Dornikov et al., 1995). Also, $\sigma$:

$$\sigma = (K_1 k_o^{0.5})/ (K_o k_1^{0.5}) = 0.865 \quad \textbf{(19)}$$

$K_1$ = thermal conductivity of gabbro = 0.0043

$k_1$ = diffusivity of gabbro = 0.008
$K_o$ = thermal conductivity of quartzite and shale = (0.0128 + 0.0019)/2 = 0.00735
$k_o$ = diffusivity of quartzite and shale = (0.031 + 0.004)/2 = 0.0175

Assuming a latent heat of fusion of 418 J/gm; the estimated temperature at the contact is raised by ~100°C to 768°C, which is ~70°C higher than the $\Delta^{18}O$ (Qt-Mt) temperature at the contact in Fig. 6. To make the predicted contact metamorphic thermal profile, temperatures were calculated (Appendix 4; Jaeger's Fig. 1 (1959) of $T_m/T_{contact}$ vs. X/D; Jaeger's curve 5: assumes equal thermal properties for the country rock and magma, latent heat of fusion = 418 J/gm and $T_1$ = 1100-800°C), where $T_m$ = maximum temperature at distance X from the contact, and D is the thickness of the intrusion. The thickness is estimated at 3 km for the Duluth Complex by averaging known thicknesses to the south, (2 km; Hauk et al., 1997), and to the north, (4 km; Miller, 1999), of the study area. The assumption of equal thermal properties for the country rock and magma is a simplification; however, the thermal properties of gabbro and the layered quartzite-shale BIF are similar (see above). The change in the estimated thermal profile of the Biwabik iron-formation would be minimal if the country rock and magma were not assumed equal in thermal properties.

The predicted thermal profile for the Biwabik iron-formation is similar to the curve fit through the $\Delta^{18}O$ (Qt-Mt) data, but shows higher temperatures at the contact. Temperatures drop sharply away from the contact, but the Jaeger (1959) thermal profile predicts higher temperatures (Fig. 6). Farther away from the contact, greater than 1400 m, the calculated thermal profile is lower than the second order polynomial fit through the data (Fig. 6). The general agreement with the predicted thermal profile for the Biwabik iron-formation calculated from Jaeger (1959) and the fit curve through the data supports the thermometry of this study.

There is a possible alternative interpretation for the curve fit through the temperature data. The calculated closure temperatures are close to the temperatures from measured $\Delta^{18}O$ (Qt-Mt) thermometry suggesting another interpretation, that the temperatures record retrograde exchange along a thermal profile. Since quartz and magnetite are coarsest near contact and decrease in size away from the contact, the temperatures measured from $\Delta^{18}O$ (Qt-Mt) may actually be closure temperatures. This hypothesis suggests minerals closer to the contact may be isotopically zoned (Jaeger, 1959). If this interpretation is correct, the true temperatures would be higher than the temperatures calculated by $\Delta^{18}O$ (Qt-Mt). Detailed $\delta^{18}O$ measurements within minerals to determine whether or not they are zoned would be possible by ion microprobe analysis, but was not attempted in this study.

***Intrusion depth of the Duluth Complex***

The temperatures from this study were used to determine the depth at which the Duluth Complex was emplaced. The temperature of the grunerite isograd is 369 ±16°C, and the pressure is estimated to be 3 ±3 kb based on the dehydration reaction (9) (Fig. 7; Evans and Guggenheim, 1988). This reaction independently verifies the $\Delta^{18}O$ (Qt-Mt) temperatures, but is not very restrictive of pressure. The temperature of the fayalite isograd based on reaction (11) is 490 ±28°C for the Fe-Si-O-$H_2O$ system, yielding a lower and tighter pressure estimate of 0.6 ±0.4 kb (Fig. 7). Thus depth is best constrained by reaction (11) to indicate that the intrusion of the Duluth Complex was shallow, 2.2 ±1.5 km. However, the estimated thickness of the Duluth Complex is 3 km, which makes the intrusion depth estimate extremely shallow for a coarse grained plutonic rock. However, if Biwabik iron-formation was near the top of the Duluth Complex, this may be reasonable. To calculate the minimum

extent of the Duluth Complex above the iron-formation, the geometry of the samples furthest away from the contact was used: a dip of 60° and a 3-D distance normal to the contact of 2.7 km yields a minimum of 1.4 km of the Duluth Complex above the Biwabik iron-formation. If the remainder of the 3 km thickness of the Duluth Complex is below the iron-formation, it intruded at a very shallow depth, but not at the surface.

To estimate the relative shift of reaction (11) in Fig. 7 (Jenkins and Bozhilov, 2003) with changing Fe/Fe+Mg ratios of grunerite and fayalite, coexisting grunerite and fayalite Fe/Fe+Mg ratios were used to calculate a $K_D$. Floran and Pipike (1978) analyzed coexisting grunerite and fayalite in one sample (67-223(1)). The Fe/Fe+Mg ratio for grunerite is 0.968 and the Fe/Fe+Mg ratio for fayalite is 0.977. The $K_{D\,(Fe/Mg)}^{fayalite/grunerite}$ = (Fe/Mg) fayalite/(Fe/Mg) grunerite is 1.404. This qualitatively extends the grunerite field to higher temperatures, which would give an even lower pressure and shallower depth as estimated by the temperature for the fayalite isograd. Thus all data are consistent with pressure less than 1 kb.

The pressures estimated for the grunerite and fayalite isograds are lower than previous work estimated by temperatures and mineral assemblages of the Biwabik iron-formation (2-5 kb; French 1973); by temperatures and mineral assemblages of the Giants Range Batholith (Fig. 1) (1.5-2.5 kb; Sims and Viswanathan, 1972); and by granite mineral assemblages (1.5-3 kb; Tuttle and Bowen, 1958). In the Gunflint iron-formation to the north which the Duluth Complex also intrudes, the reaction fayalite + $O_2$ = magnetite + quartz, for which activity coefficient data define temperatures using phase equilibria, was used by Simmons et al. (1974) to calculate pressures of: 2-3 kb.

An alternate way to estimate pressure would be by pyroxene-olivine-quartz stability (equation 12). Using $\Delta^{18}O$ (Qt-Mt) temperatures near the contact of the Biwabik iron-formation and the Duluth Complex, and reported values for ferrosilite, which are 0.75-0.8 Fe (Bonnichsen, 1969), leads to estimates of pressure of 3-4 kb (Bohlen and Boettcher, 1981). To examine this method further would require detailed electron microprobe analyses.

***Oxygen Isotope Composition of the Ocean at 1.9 Ga***

Secular variation of $\delta^{18}O$ in ocean sediments through time since the Archean has been proposed (Perry, 1967; Veizer and Hoefs, 1976; Knauth and Lowe, 2003; Perry and Lefticariu, 2003) and understanding the meaning of this variation bears on interpretation of the $\delta^{18}O$ value and temperature of sea water through time. Values of $\delta^{18}O$ (Qt) and $\delta^{18}O$ (chert), using data gathered worldwide and spanning the Archean to the present has increased through time to the present (e.g. Perry 1967; Perry and Tan, 1972; Perry et al., 1973; Becker and Clayton, 1976; Perry and Ahmad, 1983; Robert et al., 1992; Winter and Knauth, 1992; Knauth and Lowe, 2003; Perry and Lefticariu, 2003). Carbonates show a trend of the same magnitude as cherts (Veizer and Hoefs, 1976; Perry and Ahmad, 1983; Veizer, 1997).

To understand Precambrian sea water $\delta^{18}O$ and implications for ocean temperature, three models must be considered for the chert data: 1) the measured $\delta^{18}O$ (Qt) values are pristine and sea water had negative $\delta^{18}O$ values in the Precambrian; 2) the measured $\delta^{18}O$ (Qt) are pristine, sea water has remained at ~0‰ since the Precambrian, and hotter sea water temperatures in the Precambrian caused lower $\delta^{18}O$ (Qt) values; and 3) $\delta^{18}O$ (Qt) values are not pristine and have been reset through alteration.

The difficulty of analyzing older rocks is that there is a greater likelihood that the rocks have been altered by exchange during diagenesis or metamorphism. The $\Delta^{18}O$ (Qt-Mt) of the Biwabik iron-formation at the time of deposition was larger because the minerals precipitated at temperature lower than the metamorphic temperature. Metamorphism decreases the $\Delta^{18}O$ (Qt-Mt) due to exchange, therefore the $\delta^{18}O$ (Qt) has been lowered and $\delta^{18}O$ (Mt) raised. To minimize the effect of metamorphic exchange, quartz is ideal. Quartz is the main mineral in the Biwabik iron-formation, therefore the largest reservoir for oxygen, in the rocks analyzed.

Ideally, the $\Delta^{18}O$ (Qt-Mt) thermometry used to calculate depositional quartz, and sea water $\delta^{18}O$ values would be equation (2) (Appendix 5). However, Clayton and Kieffer (1991) calibrations were empirically evaluated at high temperatures, greater than 600 °C, and extrapolation to temperatures below ~125°C is not recommended by Clayton and Kieffer (1991). Values of $\Delta^{18}O$ (Qt-Mt) at temperatures of 45-65°C, were calculated by subtracting $\Delta^{18}O$ (Mt-water) from $\Delta^{18}O$ (Silica-water). Both mineral-water calibrations are for low temperatures. Brandriss (1998) calculated $\Delta^{18}O$ (silica-water) thermometry (equation 4; Appendix 5) by analyzing frustrules of freshwater diatoms cultured in the laboratory at temperatures from 3.6 to 20.0 °C. Mandernack et al. (1999) calculated $\Delta^{18}O$ (Mt-water) by analyzing magnetite precipitated by magnetotactic bacteria at temperatures from 4 to 100 °C (equation 5; Appendix 5). Different calibrations for these thermometers yield different results (Appendix 5). For example, the difference between $\Delta^{18}O$ (silica-water) and $\Delta^{18}O$ (Qt-water) calibrations at low temperatures is 3-8‰ (Brandriss et al., 1998). The calibrations used in this study were chosen based on their methods and low temperature empirical work.

The temperature chosen, 55 °C, is an estimate of the ocean water temperature from which the quartz and magnetite precursors precipitated based on previous carbonate and quartz calculations of Precambrian sea water temperature (Knauth, 1998; Winhusen, 2000). The precursor for quartz in this study was likely aqueous opaline ooze, and the magnetite precursor was likely FeOOH, which through diagenesis became hematite. Assuming there has been conservation of $\delta^{18}O$ (Qt) through diagenesis and low grade metamorphism, the seawater was estimated as if quartz and magnetite were the original precipitates.

The average depositional $\delta^{18}O$ (Qt) for the less metamorphosed samples (outcrops 44-36), was 21.0‰. The values ranged from 19.9-22.9‰ which suggests original heterogeneity of the samples. If the temperature was 10°C lower during deposition, this shifts the estimated average $\delta^{18}O$ (Qt) to 21.3‰, and if the temperature was 10°C higher the average $\delta^{18}O$ (Qt) would be 20.7‰.

The calculated $\delta^{18}O$ (Qt) at 55°C was used in equation (4) (Brandriss et al., 1998) to solve for the $\delta^{18}O$ of sea water at the time of the deposition of the Biwabik iron-formation. The average $\delta^{18}O$ (sea water) for the same samples was -5.5‰. Again, if the temperature was 10°C lower during deposition, this shifts the average $\delta^{18}O$ (sea water) to -6.7‰, and if the temperature was 10°C higher the average $\delta^{18}O$ (sea water) is -4.4‰. The calculated $\delta^{18}O$ (sea water) is very low.

***Temperature of Ocean at 1.9 Ga***

It has been proposed based on ocean crust and ophiolites that the $\delta^{18}O$ of the ocean has remained constant at ~0 ±2‰ (e.g. Muehlenbachs and Clayton, 1976; Gregory and Taylor, 1981; Bowers and Taylor, 1985; Muehlenbachs, 1986; Muehlenbachs, 1998;

Muehlenbachs, 2001). If correct, then a secular change in $\delta^{18}O$ (Qt) can be explained by increased ocean temperatures in the Precambrian (Knauth and Epstein, 1976; Perry and Lefticariu, 2003). To estimate the sea water temperature at 1.9 Ga, the average $\delta^{18}O$ (Qt) measured for outcrops 44-36 was used in equation (4), assuming $\delta^{18}O$ (sea water) was zero. This yielded a temperature of sea water of 98 ±3°C, which is rather extreme since it is just below the boiling temperature for water at 1 bar. A shift in $\delta^{18}O$ of sea water would lower the estimated temperature at 1.9 Ga, but it is not likely that sea water has shifted more than ±2 ‰ (Muehlenbachs, 1998).

Perry and Lefticariu (2003) estimated the ocean temperature at 1.9 Ga using the highest quartz value because that quartz is considered the least altered. Their highest quartz, $\delta^{18}O$ (Qt) = 24‰, gives a sea water temperature at the deposition of the Biwabik of 73°C, if $\delta^{18}O$ (sea water) = 0‰. The highest depositional $\delta^{18}O$ (Qt) value of this study is 22.9‰, which gives a higher temperature of 82 °C. The reason that the $\delta^{18}O$ (Qt) value of Perry and Lefticariu (2003) is higher than this study is that in addition to the samples in Table 2, they had samples from lower grades which produced the $\delta^{18}O$ (Qt) value of 24‰. However, by choosing only the highest $\delta^{18}O$ (Qt) value as the least altered assumes that over 90% of the quartz has been reset through diagenesis or metamorphism.

The temperature calculated without a shift in sea water $\delta^{18}O$ is unlikely, suggesting that the $\delta^{18}O$ (Qt) have been altered as in model three. The quartz of the outcrops used above is fine grained. The $\delta^{18}O$ (Qt) may have exchanged during diagensis from a siliceous gel precursor to chert (Perry and Lefticariu, 2003). The temperature of this process and the composition of any fluid involved is unknown, but if exchange took place it might lower or raise the $\delta^{18}O$ (Qt). In this case, no reliable estimate of the sea water temperature or $\delta^{18}O$ is

possible. If chert precipitated directly from the ocean (Perry and Lefticariu, 2003), another way to shift the estimate of the sea water temperature is to assume groundwater mixing after crystallization or during diagenesis. This means while the average $\delta^{18}O$ sea water may have remained at zero, locally there may have been mixing to lower $\delta^{18}O$ of pore fluids. This suggests that the contact metamorphosed Biwabik iron-fromation should not be used to infer Precambrian ocean composition or temperature.

## SUMMARY

Temperatures estimated from measured $\delta^{18}O$ of quartz and magnetite, decrease from 700 °C at the contact to 370°C at 2.6 km normal to the contact. The temperatures of this study are higher than those of Perry and Bonnichsen (1966) at the contact, and lower farther from the contact. Closure temperatures of magnetite and quartz calculated for $P(H_2O)$ = 1 kb and a cooling rate of 500°C/Ma are lower than measured $\Delta^{18}O$ metamorphic temperatures at the contact (Dodson, 1973; Dennis, 1984; Giletti and Hess, 1988; Sharp et al., 1991) suggesting that the Biwabik iron-formation was dry at its contact with the Duluth Complex. The temperature of outcrops at the fayalite isograd was used to estimate the depth at which the Duluth Complex was emplaced. The pressure estimated is 0.6 ±0.4 kb based on the dehydration reaction of grunerite = fayalite + quartz + $H_2O$ (Evans and Guggenheim, 1988; Jenkins and Bozhilov, 2003). This pressure corresponds to the depth of the Duluth Complex intrusion to be 2.2 ± 1.5 km. The alteration of the Biwabik iron-formation during diagenesis and metamorphism prevents estimation of the composition or temperature of the Precambrian ocean.

**Table 1.** Distances from the contact with the Duluth Complex; $\delta^{18}O$ of magnetite and quartz, $\Delta^{18}O$ (Qt-Mt), and their respective standard deviations; temperatures; and isograd zones for samples collected in this study from the Biwabik iron-formation of Minnesota.

| Sample # | UW # 1962/ | Distance from contact (m; map) | Distance from contact (m; 3-D) | $\delta^{18}O$ (Qt) ‰ VSMOW | Qt St D | $\delta^{18}O$ (Mt) ‰ VSMOW | Mt St D | $\Delta^{18}O$ (Qt-Mt)‰ | $\Delta^{18}O$ (Qt-Mt) St D | T, °C * | Isograd zone ‡ |
|---|---|---|---|---|---|---|---|---|---|---|---|
| 03BIW 39C | 39.3 | 0 | 0 | 13.23 | 0.03 | 8.79 | 0.04 | 4.44 | 0.05 | 918 | 8 |
| 03BIW 39C | 39.3 | 0 | 0 | 13.29 | | 8.86 | | | | | 8 |
| 03BIW 40B | 40.2 | 0.5 | 0.5 | 14.87 | 0.00 | 9.26 | 0.05 | 5.56 | 0.05 | 791 | 8 |
| 03BIW 40B | 40.2 | 0.5 | 0.5 | 14.87 | | 9.37 | | | | | 8 |
| 03BIW 40A | 40.1 | 0.5 | 0.5 | 15.06 | 0.02 | 9.08 | 0.03 | 5.99 | 0.03 | 752 | 8 |
| 03BIW 40A | 40.1 | 0.5 | 0.5 | 15.03 | | 9.03 | | | | | 8 |
| 03BIW 40C | 40.3 | 0.5 | 0.5 | 15.22 | 0.05 | 8.88 | 0.01 | 6.28 | 0.05 | 728 | 8 |
| 03BIW 40C | 40.3 | 0.5 | 0.5 | 15.12 | | 8.91 | | | | | 8 |
| 03BIW 39E | 39.5 | 8 | 4 | 13.51 | 0.05 | 7.21 | 0.07 | 6.43 | 0.09 | 716 | 8 |
| 03BIW 39E | 39.5 | 8 | 4 | 13.62 | | 7.07 | | | | | 8 |
| 03BIW 39E | 39.5 | 8 | 4 | 14.00 | 0.24 | 7.39 | 0.00 | 6.37 | 0.24 | 721 | 8 |
| 03BIW 39E | 39.5 | 8 | 4 | 13.51 | | 7.39 | | | | | 8 |
| 03BIW 39D | 39.4 | 8 | 4 | 14.55 | 0.06 | 8.24 | 0.00 | 6.37 | 0.06 | 721 | 8 |
| 03BIW 39D | 39.4 | 8 | 4 | 14.67 | | 8.25 | | | | | 8 |
| 03BIW 43E | 43.5 | 10 | 5 | 12.67 | 0.11 | 6.93 | 0.06 | 5.79 | 0.13 | 769 | 8 |
| 03BIW 43E | 43.5 | 10 | 5 | 12.89 | | 7.05 | | | | | 8 |
| 03BIW 43B | 43.5 | 10 | 5 | 12.96 | 0.17 | 6.58 | 0.07 | 6.62 | 0.18 | 702 | 8 |
| 03BIW 43B | 43.5 | 10 | 5 | 13.30 | | 6.44 | | | | | 8 |
| 03BIW 43A | 43.1 | 10 | 5 | 13.64 | 0.09 | 6.90 | 0.02 | 6.63 | 0.09 | 701 | 8 |
| 03BIW 43A | 43.1 | 10 | 5 | 13.46 | | 6.95 | | | | | 8 |
| 03BIW 43D | 43.4 | 10 | 5 | 14.40 | 0.00 | 6.72 | 0.05 | 7.73 | 0.05 | 629 | 8 |
| 03BIW 43D | 43.4 | 10 | 5 | | | 6.62 | | | | | 8 |
| 03BIW 18E | 18.5 | 15 | 8 | 15.18 | 0.09 | 8.06 | 0.09 | 6.95 | 0.12 | 679 | 8 |
| 03BIW 18E | 18.5 | 15 | 8 | 15.00 | | 8.23 | | | | | 8 |
| 03BIW 18C | 18.3 | 15 | 8 | 13.95 | 0.00 | 6.58 | 0.11 | 7.47 | 0.11 | 644 | 8 |
| 03BIW 18C | 18.3 | 15 | 8 | 13.94 | | 6.37 | | | | | 8 |
| 03BIW 18B | 18.2 | 15 | 8 | 13.76 | 0.02 | 7.31 | 0.24 | 6.76 | 0.25 | 691 | 8 |
| 03BIW 18B | 18.2 | 15 | 8 | 13.80 | | 6.75 | | | | | 8 |
| 03BIW 18B | 18.2 | 15 | 8 | | | 7.11 | | | | | 8 |
| 03BIW 18B | 18.2 | 15 | 8 | | | 6.90 | | | | | 8 |
| 03BIW 17E | 17.5 | 20 | 10 | 12.51 | 0.29 | 7.17 | 0.17 | 5.80 | 0.34 | 768 | 8 |
| 03BIW 17E | 17.5 | 20 | 10 | 13.09 | | 6.83 | | | | | 8 |
| 03BIW 17D | 17.4 | 20 | 10 | 13.94 | 0 | 6.94 | 0.02 | 6.99 | 0.02 | 676 | 8 |
| 03BIW 17D | 17.4 | 20 | 10 | | | 6.97 | | | | | 8 |
| 03BIW 17B | 17.2 | 20 | 10 | 12.45 | 0.03 | 4.47 | 0.00 | 7.96 | 0.03 | 616 | 8 |
| 03BIW 17B | 17.2 | 20 | 10 | 12.39 | | 4.46 | | | | | 8 |
| 03BIW 17C | 17.3 | 20 | 10 | 12.32 | 0.00 | 6.18 | 0.05 | 6.19 | 0.05 | 735 | 8 |
| 03BIW 17C | 17.3 | 20 | 10 | 12.32 | | 6.08 | | | | | 8 |
| 03BIW 2B | 2.2 | 16 | 9 | 12.10 | 0.30 | 4.92 | 0.00 | 7.48 | 0.30 | 644 | 8 |
| 03BIW 2B | 2.2 | 16 | 9 | 12.70 | | | | | | | 8 |
| 03BIW 12C | 12.3 | 40 | 20 | 13.69 | 0.04 | 7.34 | 0.04 | 6.35 | 0.06 | 722 | 8 |
| 03BIW 12C | 12.3 | 40 | 20 | 13.77 | | 7.42 | | | | | 8 |
| 03BIW 12D | 12.4 | 40 | 20 | 13.42 | 0.17 | 7.13 | 0.21 | 6.67 | 0.27 | 698 | 8 |
| 03BIW 12D | 12.4 | 40 | 20 | 13.75 | | 6.71 | | | | | 8 |
| 03BIW 12B | 12.2 | 40 | 20 | 13.30 | 0.01 | 7.10 | 0.04 | 6.16 | 0.04 | 737 | 8 |
| 03BIW 12B | 12.2 | 40 | 20 | 13.29 | | 7.17 | | | | | 8 |
| 03BIW 6A | 6.1 | 60 | 30 | 14.59 | 0.00 | 6.62 | 0.07 | 8.04 | 0.07 | 612 | 8 |
| 03BIW 6A | 6.1 | 60 | 30 | 14.59 | | 6.49 | | | | | 8 |
| 03BIW 6D | 6.4 | 60 | 30 | 14.12 | 0.03 | 7.06 | 0.05 | 7.09 | 0.06 | 669 | 8 |
| 03BIW 6D | 6.4 | 60 | 30 | 14.06 | | 6.95 | | | | | 8 |
| 03BIW 6C | 6.3 | 60 | 30 | 14.43 | 0.1 | 6.93 | 0.21 | 7.59 | 0.22 | 637 | 8 |
| 03BIW 6C | 6.3 | 60 | 30 | 14.56 | | 6.88 | | | | | 8 |

*Clayton and Kieffer (1991); ‡ French (1968), Frost (2001).

| Sample # | UW # 1962/ | Distance from contact (m; map) | Distance from contact (m; 3-D) | $\delta^{18}O$ (Qt) ‰ VSMOW | Qt St D | $\delta^{18}O$ (Mt) ‰ VSMOW | Mt St D | $\Delta^{18}O$ (Qt-Mt)‰ | $\Delta^{18}O$ (Qt-Mt) St D | T, °C * | Isograd zone ‡ |
|---|---|---|---|---|---|---|---|---|---|---|---|
| 03BIW 6B | 6.2 | 60 | 30 | 14.43 | 0.12 | 6.20 | 0.16 | 7.96 | 0.20 | 616 | 8 |
| 03BIW 6B | 6.2 | 60 | 30 | 14.20 | | 6.51 | | | | | 8 |
| 03BIW 6B | 6.2 | 60 | 30 | 14.36 | | 6.40 | | | | | 8 |
| 03BIW 8D | 8.4 | 55 | 28 | 14.23 | 0.05 | 6.77 | 0.08 | 7.44 | 0.09 | 647 | 8 |
| 03BIW 8D | 8.4 | 55 | 28 | 14.33 | | 6.92 | | | | | 8 |
| 03BIW 8C | 8.3 | 55 | 28 | 14.66 | 0.01 | 7.17 | 0.04 | 7.54 | 0.04 | 640 | 8 |
| 03BIW 8C | 8.3 | 55 | 28 | 14.69 | | 7.10 | | | | | 8 |
| 03BIW 3E | 3.5 | 65 | 33 | 13.13 | 0.02 | 6.32 | 0.20 | 7.03 | 0.20 | 673 | 8 |
| 03BIW 3E | 3.5 | 65 | 33 | 13.17 | | 5.93 | | | | | 8 |
| 03BIW 3A | 3.1 | 65 | 33 | 11.15 | 0.00 | 3.68 | 0.02 | 7.46 | 0.02 | 645 | 8 |
| 03BIW 3A | 3.1 | 65 | 33 | | | 3.71 | | | | | 8 |
| 03BIW 3B | 3.2 | 65 | 33 | 11.51 | 0.00 | 5.11 | 0.05 | 6.45 | 0.05 | 714 | 8 |
| 03BIW 3B | 3.2 | 65 | 33 | | | 5.01 | | | | | 8 |
| 03BIW 3C | 3.3 | 65 | 33 | 14.81 | 0.17 | 7.33 | 0.03 | 7.68 | 0.17 | 632 | 8 |
| 03BIW 3C | 3.3 | 65 | 33 | 15.15 | | 7.27 | | | | | 8 |
| 03BIW 10A | 10.1 | 35 | 18 | 12.43 | 0.01 | 5.88 | 0.01 | 6.58 | 0.02 | 705 | 8 |
| 03BIW 10A | 10.1 | 35 | 18 | 12.46 | | 5.86 | | | | | 8 |
| 03BIW 10C | 10.3 | 35 | 18 | 13.41 | 0.04 | 6.47 | 0.03 | 6.87 | 0.05 | 684 | 8 |
| 03BIW 10C | 10.3 | 35 | 18 | 13.32 | | 6.53 | | | | | 8 |
| 03BIW 22C | 22.3 | 200 | 100 | 13.85 | 0.02 | 7.62 | 0.00 | 6.26 | 0.02 | 729 | 8 |
| 03BIW 22C | 22.3 | 200 | 100 | 13.90 | | 7.62 | | | | | 8 |
| 03BIW 22B | 22.2 | 200 | 100 | 14.50 | 0.01 | 7.46 | 0.04 | 7.01 | 0.04 | 674 | 8 |
| 03BIW 22B | 22.2 | 200 | 100 | 14.52 | | 7.54 | | | | | 8 |
| 03BIW 22E | 22.5 | 200 | 100 | 14.47 | 0.00 | 7.59 | 0.01 | 6.89 | 0.01 | 682 | 8 |
| 03BIW 22E | 22.5 | 200 | 100 | | | 7.57 | | | | | 8 |
| 03BIW 22D | 22.4 | 200 | 100 | 14.21 | 0.15 | 7.83 | 0.18 | 6.70 | 0.23 | 696 | 8 |
| 03BIW 22D | 22.4 | 200 | 100 | 14.50 | | 7.48 | | | | | 8 |
| 03BIW 23B-1 | 23.2a | 210 | 105 | 14.37 | 0.08 | 7.75 | 0.13 | 6.58 | 0.15 | 705 | 8 |
| 03BIW 23B-1 | 23.2a | 210 | 105 | 14.53 | | 8.00 | | | | | 8 |
| 03BIW 23B-1 | 23.2a | 210 | 105 | | | 7.86 | | | | | 8 |
| 03BIW 23E | 23.5 | 210 | 105 | 14.40 | 0.07 | 7.36 | 0.15 | 6.82 | 0.17 | 687 | 8 |
| 03BIW 23E | 23.5 | 210 | 105 | 14.26 | | 7.66 | | | | | 8 |
| 03BIW 23A | 23.1 | 210 | 105 | 14.77 | 0.18 | 7.68 | 0.01 | 6.91 | 0.18 | 681 | 8 |
| 03BIW 23A | 23.1 | 210 | 105 | 14.42 | | 7.69 | | | | | 8 |
| 03BIW 23B-2 | 23.2b | 210 | 105 | 14.61 | 0.07 | 7.51 | 0.05 | 7.11 | 0.08 | 668 | 8 |
| 03BIW 23B-2 | 23.2b | 210 | 105 | 14.52 | | 7.41 | | | | | 8 |
| 03BIW 27A | 27.1 | 300 | 150 | 14.69 | 0.06 | 7.79 | 0.11 | 6.73 | 0.13 | 694 | 8 |
| 03BIW 27A | 27.1 | 300 | 150 | 14.56 | | 8.01 | | | | | 8 |
| 03BIW 27B | 27.2 | 300 | 150 | 15.17 | 0.03 | 6.49 | 0.03 | 8.62 | 0.05 | 581 | 8 |
| 03BIW 27B | 27.2 | 300 | 150 | 15.11 | | 6.56 | | | | | 8 |
| 03BIW 30D | 30.4 | 325 | 163 | 13.16 | 0.09 | 5.42 | 0.10 | 7.73 | 0.13 | 629 | 8 |
| 03BIW 30D | 30.4 | 325 | 163 | 13.34 | | 5.62 | | | | | 8 |
| 03BIW 31D | 31.4 | 220 | 110 | 14.97 | 0.00 | 8.28 | 0.13 | 6.70 | 0.13 | 696 | 8 |
| 03BIW 31D | 31.4 | 220 | 110 | | | 8.23 | | | | | 8 |
| 03BIW 31D | 31.4 | 220 | 110 | | | 8.44 | | | | | 8 |
| 03BIW 31D | 31.4 | 220 | 110 | | | 8.12 | | | | | 8 |
| 03BIW 31A | 31.1 | 220 | 110 | 14.66 | 0.01 | 7.66 | 0.12 | 6.87 | 0.12 | 684 | 8 |
| 03BIW 31A | 31.1 | 220 | 110 | 14.64 | | 7.90 | | | | | 8 |
| 03BIW 31C | 31.3 | 220 | 110 | 14.45 | 0.32 | 8.72 | 0.82 | 6.87 | 0.88 | 684 | 8 |
| 03BIW 31C | 31.3 | 220 | 110 | 15.09 | | 7.08 | | | | | 8 |
| 03BIW 32B | 32.2 | 330 | 170 | 14.12 | 0.08 | 6.08 | 0.13 | 8.24 | 0.15 | 601 | 7 |
| 03BIW 32B | 32.2 | 330 | 170 | 14.27 | | 5.83 | | | | | 7 |

*Clayton and Kieffer (1991); ‡ French (1968), Frost (2001).

| Sample # | UW # 1962/ | Distance from contact (m; map) | Distance from contact (m; 3-D) | $\delta^{18}O$ (Qt) ‰ VSMOW | Qt St D | $\delta^{18}O$ (Mt) ‰ VSMOW | Mt St D | $\Delta^{18}O$ (Qt Mt)‰ | $\Delta^{18}O$ (Qt-Mt) St D | T, °C * | Isograd zone ‡ |
|---|---|---|---|---|---|---|---|---|---|---|---|
| 03BIW 44B-1 | 44.2a | 2500 | 1250 | 16.25 | 0.17 | 5.08 | 0.04 | 11.04 | 0.17 | 482 | 7 |
| 03BIW 44B-1 | 44.2a | 2500 | 1250 | 15.91 | | 5.01 | | | | | 7 |
| 03BIW 44D | 44.4 | 2500 | 1250 | 16.72 | 0.04 | 6.07 | 0.00 | 10.69 | 0.04 | 494 | 7 |
| 03BIW 44D | 44.4 | 2500 | 1250 | 16.80 | | | | | | | 7 |
| 03BIW 44C | 44.3 | 2500 | 1250 | 16.58 | 0.17 | 6.57 | 0.56 | 10.04 | 0.58 | 518 | 7 |
| 03BIW 44C | 44.3 | 2500 | 1250 | 16.92 | | 6.66 | | | | | 7 |
| 03BIW 44C; M1 | 44.3 | 2500 | 1250 | | | 6.07 | | | | | 7 |
| 03BIW 44C; M1 | 44.3 | 2500 | 1250 | | | 7.76 | | | | | 7 |
| 03BIW 44C; M2 | 44.3 | 2500 | 1250 | | | 6.61 | | | | | 7 |
| 03BIW 44C; M2 | 44.3 | 2500 | 1250 | | | 6.63 | | | | | 7 |
| 03BIW 44A | 44.1 | 2500 | 1250 | 17.38 | 0.15 | 6.52 | 0.06 | 10.77 | 0.17 | 491 | 7 |
| 03BIW 44A | 44.1 | 2500 | 1250 | 17.07 | | 6.39 | | | | | 7 |
| 03BIW 34B | 34.2 | 3000 | 2598 | 17.18 | 0.09 | 1.59 | 0.00 | 15.68 | 0.09 | 360 | 3 |
| 03BIW 34B | 34.2 | 3000 | 2598 | 17.36 | | 1.59 | | | | | 3 |
| 03BIW 34A | 34.1 | 3000 | 2598 | 17.01 | 0.01 | 1.77 | 0.11 | 15.41 | 0.12 | 366 | 3 |
| 03BIW 34A | 34.1 | 3000 | 2598 | 16.99 | | 1.59 | | | | | 3 |
| 03BIW 34A | 34.1 | 3000 | 2598 | | | 1.65 | | | | | 3 |
| 03BIW 34A | 34.1 | 3000 | 2598 | | | 1.35 | | | | | 3 |
| 03BIW 34E | 34.5 | 3000 | 2598 | 17.11 | 0.00 | 1.94 | 0.01 | 15.17 | 0.01 | 371 | 3 |
| 03BIW 34E | 34.5 | 3000 | 2598 | | | 1.95 | | | | | 3 |
| 03BIW 34D | 34.4 | 3000 | 2598 | 17.34 | 0.04 | 2.05 | 0.26 | 15.59 | 0.26 | 362 | 3 |
| 03BIW 34D | 34.4 | 3000 | 2598 | 17.43 | | 1.54 | | | | | 3 |
| 03BIW 34C | 34.3 | 3000 | 2598 | 16.91 | 0.04 | 2.90 | 0.27 | 14.23 | 0.27 | 392 | 3 |
| 03BIW 34C | 34.3 | 3000 | 2598 | 16.82 | | 2.37 | | | | | 3 |
| 03BIW 35A-1 | 35.1a | 3100 | 2685 | 18.86 | 0.03 | 5.93 | 0.34 | 12.50 | 0.34 | 436 | 2 |
| 03BIW 35A-1 | 35.1a | 3100 | 2685 | 18.80 | | 6.74 | | | | | 2 |
| 03BIW 35A-2 | 35.1b | 3100 | 2685 | 18.09 | 0.17 | 3.24 | 0.46 | 15.48 | 0.49 | 364 | 2 |
| 03BIW 35A-2 | 35.1b | 3100 | 2685 | 18.43 | | 2.32 | | | | | 2 |
| 03BIW 35B-1 | 35.2a | 3100 | 2685 | 19.12 | 0.07 | -1.47 | 0.65 | 21.30 | 0.65 | 270 | 2 |
| 03BIW 35B-1 | 35.2a | 3100 | 2685 | 19.26 | | -2.76 | | | | | 2 |
| 03BIW 35E | 35.5 | 3100 | 2685 | 18.86 | 0.07 | -6.22 | 1.64 | 24.79 | 1.64 | 231 | 2 |
| 03BIW 35E | 35.5 | 3100 | 2685 | 19.00 | | -6.30 | | | | | 2 |
| 03BIW 35E; M1 | 35.5 | 3100 | 2685 | | | -5.91 | | | | | 2 |
| 03BIW 35E; M2 | 35.5 | 3100 | 2685 | | | -8.11 | | | | | 2 |
| 03BIW 35E; M2 | 35.5 | 3100 | 2685 | | | -7.04 | | | | | 2 |
| 03BIW 35E; M3 | 35.5 | 3100 | 2685 | | | -3.85 | | | | | 2 |
| 03BIW 35E; M3 | 35.5 | 3100 | 2685 | | | -3.56 | | | | | 2 |
| 03BIW 35B-2 | 35.2b | 3100 | 2685 | 19.00 | 0.00 | -5.95 | 0.59 | 23.78 | 0.59 | 241 | 2 |
| 03BIW 35B-2 | 35.2b | 3100 | 2685 | 19.00 | | -4.90 | | | | | 2 |
| 03BIW 35B-2 | 35.2b | 3100 | 2685 | | | -5.03 | | | | | 2 |
| 03BIW 35B-2 | 35.2b | 3100 | 2685 | | | -3.85 | | | | | 2 |
| 03BIW 35B-2; M1 | 35.2b | 3100 | 2685 | | | -4.65 | | | | | 2 |
| 03BIW 35B-2; M1 | 35.2b | 3100 | 2685 | | | -4.06 | | | | | 2 |
| 03BIW 35B-2; M2 | 35.2b | 3100 | 2685 | | | -6.19 | | | | | 2 |
| 03BIW 35B-2; M2 | 35.2b | 3100 | 2685 | | | -4.76 | | | | | 2 |
| 03BIW 35B-2; M3 | 35.2b | 3100 | 2685 | | | -4.68 | | | | | 2 |
| 03BIW 35B-2; M3 | 35.2b | 3100 | 2685 | | | -3.72 | | | | | 2 |

*Clayton and Kieffer (1991); ‡ French (1968), Frost (2001).

| Sample # | UW # 1962/ | Distance from contact (m; map) | Distance from contact (m; 3-D) | $\delta^{18}O$ (Qt) ‰ VSMOW | Qt St D | $\delta^{18}O$ (Mt) ‰ VSMOW | Mt St D | $\Delta^{18}O$ (Qt-Mt)‰ | $\Delta^{18}O$ (Qt-Mt) St D | T, °C * | Isograd zone ‡ |
|---|---|---|---|---|---|---|---|---|---|---|---|
| 03BIW 36M | 36.13 | 3150 | 2728 | 18.86 | 0.07 | -2.70 | 0.72 | 21.00 | 0.72 | 274 | 2 |
| 03BIW 36M | 36.13 | 3150 | 2728 | 18.72 | | -3.10 | | | | | 2 |
| 03BIW 36M; M1 | 36.13 | 3150 | 2728 | | | -1.48 | | | | | 2 |
| 03BIW 36M; M1 | 36.13 | 3150 | 2728 | | | -2.91 | | | | | 2 |
| 03BIW 36M; M2 | 36.13 | 3150 | 2728 | | | -1.72 | | | | | 2 |
| 03BIW 36M; M2 | 36.13 | 3150 | 2728 | | | -1.14 | | | | | 2 |
| 03BIW 36M; M3 | 36.13 | 3150 | 2728 | | | -2.60 | | | | | 2 |
| 03BIW 36M; M3 | 36.13 | 3150 | 2728 | | | -2.00 | | | | | 2 |

*Clayton and Kieffer (1991); ‡ French (1968), Frost (2001).

**Table 2.** Correction of $\delta^{18}O$ in cut pieces of magnetite for silicate impurity (see text). Measured and calculated $\delta^{18}O$ values, starting mass and mass after HCl dissolution, Wt %, mol fraction oxygen, and corrected magnetite $\delta^{18}O$ values. Qt = quartz, Mt = magnetite, Di = diopside, and VSMOW = Vienna standard mean ocean water.

| Sample 03-BIW- | Measured $\delta^{18}O$ (Qt) ‰ VSMOW | Measured $\delta^{18}O$ (Mt) ‰ VSMOW | Calculated $\delta^{18}O$ (Di) ‰ | Start mass (mg) | End mass (mg) | Wt% Mt | Wt% Di | Wt% Qt | Mol Fraction Oxygen (Mt) | Mol fraction Oxygen (Di) | Mol fraction oxygen (Qt) | Corrected $\delta^{18}O$ (Mt)‰ |
|---|---|---|---|---|---|---|---|---|---|---|---|---|
| 22B | 14.51 | 7.78 | 11.57 | 2.95 | 0.10 | 96.65 | 2.35 | 1.01 | 0.93 | 0.05 | 0.02 | 7.46 |
| 22B | 14.51 | 7.86 | 11.61 | 2.95 | 0.10 | 96.65 | 2.35 | 1.01 | 0.93 | 0.05 | 0.02 | 7.54 |
| 22C | 13.88 | 7.68 | 11.17 | 14.99 | 0.14 | 99.08 | 0.92 | 0.00 | 0.98 | 0.02 | 0.00 | 7.62 |
| 22C | 13.88 | 7.68 | 11.17 | 14.99 | 0.14 | 99.08 | 0.92 | 0.00 | 0.98 | 0.02 | 0.00 | 7.62 |
| 22D | 14.36 | 7.86 | 11.52 | 4.29 | 0.02 | 99.63 | 0.37 | 0.00 | 0.99 | 0.01 | 0.00 | 7.83 |
| 22D | 14.36 | 7.51 | 11.36 | 4.29 | 0.02 | 99.63 | 0.37 | 0.00 | 0.99 | 0.01 | 0.00 | 7.48 |
| 22E | 14.42 | 7.60 | 11.44 | 12.78 | 0.04 | 99.66 | 0.20 | 0.00 | 1.00 | 0.00 | 0.00 | 7.59 |
| 22E | 14.42 | 7.58 | 11.43 | 12.78 | 0.04 | 99.66 | 0.20 | 0.00 | 1.00 | 0.00 | 0.00 | 7.57 |
| 23A | 14.60 | 7.68 | 11.57 | 23.57 | 0.02 | 99.92 | 0.08 | 0.00 | 1.00 | 0.00 | 0.00 | 7.68 |
| 23A | 14.60 | 7.69 | 11.58 | 23.57 | 0.02 | 99.92 | 0.08 | 0.00 | 1.00 | 0.00 | 0.00 | 7.69 |
| 23B-1 | 14.45 | 8.11 | 11.68 | 17.93 | 0.27 | 98.51 | 1.49 | 0.00 | 0.97 | 0.03 | 0.00 | 8.00 |
| 23B-1 | 14.45 | 7.97 | 11.62 | 17.93 | 0.27 | 98.51 | 1.49 | 0.00 | 0.97 | 0.03 | 0.00 | 7.86 |
| 23B-1 | 14.45 | 7.87 | 11.57 | 17.93 | 0.27 | 98.51 | 1.49 | 0.00 | 0.97 | 0.03 | 0.00 | 7.75 |
| 23B-2 | 14.53 | 7.54 | 11.48 | 8.51 | 0.04 | 99.54 | 0.46 | 0.00 | 0.99 | 0.01 | 0.00 | 7.51 |
| 23B-2 | 14.53 | 7.45 | 11.44 | 8.51 | 0.04 | 99.54 | 0.46 | 0.00 | 0.99 | 0.01 | 0.00 | 7.41 |
| 23E | 14.33 | 7.41 | 11.30 | 10.18 | 0.06 | 99.46 | 0.32 | 0.22 | 0.99 | 0.01 | 0.00 | 7.36 |
| 23E | 14.33 | 7.71 | 11.44 | 10.18 | 0.06 | 99.46 | 0.32 | 0.22 | 0.99 | 0.01 | 0.00 | 7.66 |
| 27A | 14.63 | 8.42 | 11.91 | 2.90 | 0.24 | 91.91 | 8.09 | 0.00 | 0.85 | 0.15 | 0.00 | 7.79 |
| 27A | 14.63 | 8.62 | 12.00 | 2.90 | 0.24 | 91.91 | 8.09 | 0.00 | 0.85 | 0.15 | 0.00 | 8.01 |
| 27B | 15.14 | 7.00 | 11.58 | 3.66 | 0.19 | 94.83 | 5.17 | 0.00 | 0.90 | 0.10 | 0.00 | 6.49 |
| 27B | 15.14 | 7.07 | 11.61 | 3.66 | 0.19 | 94.80 | 5.20 | 0.00 | 0.90 | 0.10 | 0.00 | 6.56 |
| 30D | 13.25 | 5.65 | 9.93 | 4.67 | 0.10 | 97.95 | 1.23 | 0.82 | 0.96 | 0.02 | 0.02 | 5.42 |
| 30D | 13.25 | 5.85 | 10.02 | 4.67 | 0.10 | 97.95 | 1.23 | 0.82 | 0.96 | 0.02 | 0.02 | 5.62 |
| 31A | 14.65 | 7.73 | 11.63 | 3.34 | 0.02 | 99.52 | 0.34 | 0.34 | 0.99 | 0.01 | 0.01 | 7.66 |
| 31A | 14.65 | 7.97 | 11.73 | 3.34 | 0.02 | 99.52 | 0.34 | 0.34 | 0.99 | 0.01 | 0.01 | 7.90 |

| Sample 03-BIW- | Measured $\delta^{18}O$ (Qt) ‰ VSMOW | Measured $\delta^{18}O$ (Mt) ‰ VSMOW | Calculated $\delta^{18}O$ (Di) ‰ | Start mass (mg) | End mass (mg) | Wt% Mt | Wt% Di | Wt% Qt | Mol Fraction Oxygen (Mt) | Mol fraction Oxygen (Di) | Mol fraction oxygen (Qt) | Corrected $\delta^{18}O$ (Mt)‰ |
|---|---|---|---|---|---|---|---|---|---|---|---|---|
| 31C | 14.77 | 9.97 | 12.67 | 6.87 | 1.08 | 84.23 | 11.04 | 4.73 | 0.73 | 0.20 | 0.08 | 8.72 |
| 31C | 14.77 | 8.67 | 12.10 | 6.87 | 1.08 | 84.23 | 11.04 | 4.73 | 0.73 | 0.20 | 0.08 | 7.08 |
| 31D | 14.97 | 8.39 | 12.09 | 4.70 | 0.07 | 98.55 | 1.45 | 0.00 | 0.97 | 0.03 | 0.00 | 8.28 |
| 31D | 14.97 | 8.34 | 12.07 | 4.70 | 0.07 | 98.55 | 1.45 | 0.00 | 0.97 | 0.03 | 0.00 | 8.23 |
| 31D; M1 | 14.97 | 8.55 | 12.16 | 4.70 | 0.07 | 98.55 | 1.45 | 0.00 | 0.97 | 0.03 | 0.00 | 8.44 |
| 31D; M1 | 14.97 | 8.22 | 12.02 | 4.70 | 0.07 | 98.55 | 1.45 | 0.00 | 0.97 | 0.03 | 0.00 | 8.12 |
| 32B | 14.20 | 6.57 | 10.86 | 11.73 | 0.61 | 94.79 | 5.21 | 0.00 | 0.90 | 0.10 | 0.00 | 6.08 |
| 32B | 14.20 | 6.33 | 10.76 | 11.73 | 0.61 | 94.79 | 5.21 | 0.00 | 0.90 | 0.10 | 0.00 | 5.83 |
| 44A | 17.23 | 7.23 | 12.86 | 6.13 | 0.35 | 94.22 | 5.78 | 0.00 | 0.89 | 0.11 | 0.00 | 6.52 |
| 44A | 17.23 | 7.11 | 12.81 | 6.13 | 0.35 | 94.22 | 5.78 | 0.00 | 0.89 | 0.11 | 0.00 | 6.39 |
| 44B-1 | 16.08 | 6.01 | 11.68 | 2.64 | 0.16 | 93.79 | 4.34 | 1.86 | 0.88 | 0.08 | 0.03 | 5.08 |
| 44B-1 | 16.08 | 5.94 | 11.65 | 2.64 | 0.16 | 93.79 | 4.34 | 1.86 | 0.88 | 0.08 | 0.03 | 5.01 |
| 44C | 16.75 | 6.90 | 12.45 | 7.77 | 0.22 | 97.19 | 2.81 | 0.00 | 0.94 | 0.06 | 0.00 | 6.57 |
| 44C | 16.75 | 6.98 | 12.48 | 7.77 | 0.22 | 97.19 | 2.81 | 0.00 | 0.94 | 0.06 | 0.00 | 6.66 |
| 44C; M1 | 16.75 | 6.70 | 12.36 | 13.99 | 0.72 | 94.86 | 5.14 | 0.00 | 0.90 | 0.10 | 0.00 | 6.07 |
| 44C; M1 | 16.75 | 8.29 | 13.05 | 13.99 | 0.72 | 94.86 | 5.14 | 0.00 | 0.90 | 0.10 | 0.00 | 7.76 |
| 44C; M2 | 16.75 | 7.46 | 12.69 | 6.34 | 0.47 | 92.65 | 7.35 | 0.00 | 0.86 | 0.14 | 0.00 | 6.61 |
| 44C; M2 | 16.75 | 7.48 | 12.70 | 6.34 | 0.47 | 92.65 | 7.35 | 0.00 | 0.86 | 0.14 | 0.00 | 6.63 |
| 44D | 16.76 | 6.52 | 12.29 | 7.79 | 0.29 | 96.33 | 3.67 | 0.00 | 0.93 | 0.07 | 0.00 | 6.07 |
| 34A | 17.00 | 4.38 | 11.49 | 9.06 | 1.37 | 84.85 | 15.15 | 0.00 | 0.73 | 0.27 | 0.00 | 1.77 |
| 34A | 17.00 | 4.23 | 11.42 | 9.06 | 1.37 | 84.85 | 15.15 | 0.00 | 0.73 | 0.27 | 0.00 | 1.59 |
| 34A; M1 | 17.00 | 3.77 | 11.22 | 3.41 | 0.41 | 87.88 | 12.12 | 0.00 | 0.78 | 0.22 | 0.00 | 1.65 |
| 34A; M1 | 17.00 | 3.51 | 11.10 | 3.41 | 0.41 | 87.88 | 12.12 | 0.00 | 0.78 | 0.22 | 0.00 | 1.35 |
| 34B | 17.27 | 2.49 | 10.81 | 6.93 | 0.35 | 94.98 | 5.02 | 0.00 | 0.90 | 0.10 | 0.00 | 1.59 |
| 34B | 17.27 | 2.49 | 10.81 | 6.93 | 0.35 | 94.98 | 5.02 | 0.00 | 0.90 | 0.10 | 0.00 | 1.59 |
| 34C | 16.87 | 5.09 | 11.72 | 5.31 | 0.73 | 86.19 | 13.81 | 0.00 | 0.75 | 0.25 | 0.00 | 2.90 |
| 34C | 16.87 | 4.64 | 11.52 | 5.31 | 0.73 | 86.19 | 13.81 | 0.00 | 0.75 | 0.25 | 0.00 | 2.37 |
| 34D | 17.38 | 4.74 | 11.85 | 3.79 | 0.59 | 84.50 | 15.50 | 0.00 | 0.73 | 0.27 | 0.00 | 2.05 |
| 34D | 17.38 | 4.33 | 11.67 | 3.79 | 0.59 | 84.50 | 15.50 | 0.00 | 0.73 | 0.27 | 0.00 | 1.54 |
| 34E | 17.11 | 4.63 | 11.66 | 18.35 | 2.88 | 84.31 | 15.69 | 0.00 | 0.72 | 0.28 | 0.00 | 1.94 |
| 34E | 17.11 | 4.64 | 11.66 | 18.35 | 2.88 | 84.31 | 15.69 | 0.00 | 0.72 | 0.28 | 0.00 | 1.95 |
| 35A-1 | 18.83 | 7.17 | 13.73 | 3.66 | 0.29 | 92.09 | 7.12 | 0.79 | 0.85 | 0.14 | 0.01 | 5.93 |
| 35A-1 | 18.83 | 7.90 | 14.05 | 3.66 | 0.29 | 92.09 | 7.12 | 0.79 | 0.85 | 0.14 | 0.01 | 6.74 |
| 35A-2 | 18.26 | 4.60 | 12.29 | 13.57 | 1.07 | 92.09 | 7.91 | 0.00 | 0.85 | 0.15 | 0.00 | 3.24 |
| 35A-2 | 18.26 | 3.77 | 11.93 | 13.57 | 1.07 | 92.09 | 7.91 | 0.00 | 0.85 | 0.15 | 0.00 | 2.32 |

| Sample 03-BIW- | Measured $\delta^{18}O$ (Qt) ‰ VSMOW | Measured $\delta^{18}O$ (Mt) ‰ VSMOW | Calculated $\delta^{18}O$ (Di) ‰ | Start mass (mg) | End mass (mg) | Wt% Mt | Wt% other minerals | Wt% Qt | Mol Fraction Oxygen (Mt) | Mol fraction Oxygen (Di) | Mol fraction oxygen (Qt) | Corrected $\delta^{18}O$ (Mt)‰ |
|---|---|---|---|---|---|---|---|---|---|---|---|---|
| 35B-1 | 19.19 | 0.08 | 10.83 | 8.58 | 0.56 | 93.46 | 6.54 | 0.00 | 0.87 | 0.13 | 0.00 | -1.47 |
| 35B-1 | 19.19 | -1.12 | 10.31 | 8.58 | 0.56 | 93.46 | 6.54 | 0.00 | 0.87 | 0.13 | 0.00 | -2.76 |
| 35B-2 | 19.00 | -2.43 | 9.63 | 4.53 | 0.36 | 91.96 | 5.63 | 2.41 | 0.85 | 0.11 | 0.04 | -5.95 |
| 35B-2 | 19.00 | -1.37 | 10.10 | 4.53 | 0.36 | 91.96 | 5.63 | 2.41 | 0.85 | 0.11 | 0.04 | -4.90 |
| 35B-2 | 19.00 | -3.25 | 9.27 | 4.53 | 0.36 | 91.96 | 5.63 | 2.41 | 0.85 | 0.11 | 0.04 | -5.03 |
| 35B-2 | 19.00 | -2.31 | 9.69 | 4.53 | 0.36 | 91.96 | 5.63 | 2.41 | 0.85 | 0.11 | 0.04 | -3.85 |
| 35B-2 M1 | 19.00 | -3.44 | 9.19 | 9.42 | 0.42 | 95.54 | 4.46 | 0.00 | 0.91 | 0.09 | 0.00 | -4.65 |
| 35B-2 M1 | 19.00 | -2.88 | 9.44 | 9.42 | 0.42 | 95.54 | 4.46 | 0.00 | 0.91 | 0.09 | 0.00 | -4.06 |
| 35B-2 M2 | 19.00 | -2.67 | 9.53 | 3.28 | 0.36 | 88.99 | 8.81 | 2.20 | 0.80 | 0.16 | 0.04 | -6.19 |
| 35B-2 M2 | 19.00 | -1.44 | 10.07 | 3.28 | 0.36 | 88.99 | 8.81 | 2.20 | 0.80 | 0.16 | 0.04 | -4.76 |
| 35B-2 M3 | 19.00 | -3.46 | 9.18 | 4.67 | 0.19 | 96.03 | 3.17 | 0.79 | 0.92 | 0.06 | 0.01 | -4.68 |
| 35B-2 M3 | 19.00 | -2.55 | 9.58 | 4.67 | 0.19 | 96.03 | 3.17 | 0.79 | 0.92 | 0.06 | 0.01 | -3.72 |
| 35E | 18.93 | -4.18 | 8.83 | 5.86 | 0.29 | 95.05 | 1.48 | 3.46 | 0.91 | 0.03 | 0.06 | -6.22 |
| 35E | 18.93 | -4.25 | 8.80 | 5.86 | 0.29 | 95.05 | 1.48 | 3.46 | 0.91 | 0.03 | 0.06 | -6.30 |
| 35E; M1 | 18.93 | -5.28 | 8.35 | 4.23 | 0.09 | 97.94 | 1.85 | 0.21 | 0.96 | 0.04 | 0.00 | -5.91 |
| 35E; M2 | 18.93 | -3.84 | 8.97 | 3.45 | 0.43 | 87.49 | 10.01 | 2.50 | 0.77 | 0.18 | 0.04 | -8.11 |
| 35E; M2 | 18.93 | -2.94 | 9.37 | 3.45 | 0.43 | 87.49 | 10.01 | 2.50 | 0.77 | 0.18 | 0.04 | -7.04 |
| 35E; M3 | 18.93 | -3.35 | 9.19 | 14.02 | 0.25 | 98.22 | 1.60 | 0.18 | 0.96 | 0.03 | 0.00 | -3.85 |
| 35E; M3 | 18.93 | -3.07 | 9.31 | 14.02 | 0.25 | 98.22 | 1.60 | 0.18 | 0.96 | 0.03 | 0.00 | -3.56 |
| 36M | 18.79 | -2.50 | 9.48 | 9.11 | 0.07 | 99.19 | 0.81 | 0.00 | 0.98 | 0.02 | 0.00 | -2.70 |
| 36M | 18.79 | -2.89 | 9.31 | 9.11 | 0.07 | 99.19 | 0.81 | 0.00 | 0.98 | 0.02 | 0.00 | -3.10 |
| 36M; M1 | 18.79 | 0.05 | 10.60 | 0.99 | 0.06 | 93.82 | 5.56 | 0.62 | 0.88 | 0.11 | 0.01 | -1.48 |
| 36M; M1 | 18.79 | -1.28 | 10.02 | 0.99 | 0.06 | 93.82 | 5.56 | 0.62 | 0.88 | 0.11 | 0.01 | -2.91 |
| 36M; M2 | 18.79 | -1.64 | 9.86 | 13.42 | 0.05 | 99.66 | 0.34 | 0.00 | 0.99 | 0.01 | 0.00 | -1.72 |
| 36M; M2 | 18.79 | -1.06 | 10.11 | 13.42 | 0.05 | 99.66 | 0.34 | 0.00 | 0.99 | 0.01 | 0.00 | -1.14 |
| 36M; M3 | 18.79 | -2.49 | 9.49 | 9.02 | 0.04 | 99.55 | 0.45 | 0.00 | 0.99 | 0.01 | 0.00 | -2.60 |
| 36M; M3 | 18.79 | -1.89 | 9.75 | 9.02 | 0.04 | 99.55 | 0.45 | 0.00 | 0.99 | 0.01 | 0.00 | -2.00 |

**Table 3.** Calculation of $\delta^{18}O$ (whole rock) values (equation 3): $\delta^{18}O$, estimated ‰ Qt and Mt, and moles of oxygen of quartz and magnetite used to calculate the whole rock $\delta^{18}O$ values. For simplification, silicate minerals other than magnetite and quartz were calculated as quartz.

| Sample 03-BIW- | $\delta^{18}O$ Qt | $\delta^{18}O$ Mt | Estimated parts per mil Qt | Estimated parts per mil Mt | Mols/liter Oxygen (Qt) | Mols/liter Oxygen (Mt) | Whole Rock $\delta^{18}O$ |
|---|---|---|---|---|---|---|---|
| 39C | 13.26 | 8.82 | 806 | 194 | 35.53 | 8.71 | 12.38 |
| 43B | 13.13 | 6.51 | 768 | 232 | 33.85 | 10.42 | 11.58 |
| 18C | 13.95 | 6.48 | 765 | 235 | 33.70 | 10.58 | 12.16 |
| 17B | 12.42 | 4.47 | 864 | 136 | 38.10 | 6.09 | 11.32 |
| 12C | 13.73 | 7.38 | 836 | 164 | 36.85 | 7.37 | 12.67 |
| 3E | 13.15 | 6.13 | 729 | 271 | 32.13 | 12.18 | 11.22 |
| 22B | 14.51 | 7.50 | 771 | 229 | 34.00 | 10.27 | 12.89 |
| 23B-1 | 14.45 | 7.75 | 696 | 304 | 30.67 | 13.66 | 12.38 |
| 23B-2 | 14.53 | 7.46 | 833 | 167 | 36.72 | 7.50 | 13.33 |
| 31A | 14.65 | 7.78 | 848 | 152 | 37.40 | 6.81 | 13.59 |
| 31D | 14.97 | 8.26 | 816 | 184 | 35.96 | 8.27 | 13.72 |
| 44A | 17.23 | 6.46 | 652 | 348 | 28.75 | 15.62 | 13.44 |
| 34B | 17.27 | 1.59 | 711 | 289 | 31.33 | 12.99 | 12.68 |
| 34C | 16.87 | 2.64 | 551 | 449 | 24.30 | 20.16 | 10.41 |
| 34D | 17.38 | 1.80 | 662 | 338 | 29.17 | 15.19 | 12.04 |
| 34E | 17.11 | 1.95 | 650 | 350 | 28.65 | 15.72 | 11.74 |
| 35A-2 | 18.26 | 2.79 | 799 | 201 | 35.22 | 9.03 | 15.11 |
| 35B-1 | 19.19 | -2.11 | 804 | 196 | 35.44 | 8.80 | 14.95 |
| 35B-2 | 19.00 | -4.78 | 804 | 196 | 35.44 | 8.80 | 14.27 |
| 35E | 18.93 | -5.19 | 630 | 370 | 27.77 | 16.62 | 9.90 |
| 36M | 18.79 | -2.21 | 603 | 397 | 26.58 | 17.83 | 10.36 |

**Table 4.** Perry and Bonnichsen (1966) data of the Biwabik iron-formation showing distances from the contact with the Duluth Complex, $\delta^{18}O$ values of magnetite and quartz, $\Delta^{18}O$ (Qt-Mt), and the recalculated temperatures based on equation (2).

| Sample # | Distance from contact (m; 3-D) | $\delta^{18}O$ (Qt) ‰ VSMOW | $\delta^{18}O$ (Mt) ‰ VSMOW | $\Delta^{18}O$ (Qt-Mt) ‰ | T°C * |
|---|---|---|---|---|---|
| M12056 | 15 | 15.21 | 7.43 | 7.7 | 631 |
| M12022 | 52 | 12.91 | 4.69 | 8.2 | 603 |
| M12133 | 63 | 12.45 | 4.95 | 7.4 | 649 |
| M12067 | 71 | 12.64 | 4.49 | 8.1 | 608 |
| M12167 | 102 | 13.09 | 4.22 | 8.8 | 572 |
| M12232 | 128 | 13.98 | 5.49 | 8.4 | 592 |
| 36-64 | 154 | 18.90 | 9.28 | 9.5 | 541 |
| 37-64 | 171 | 12.53 | 2.49 | 10.0 | 520 |
| 38-64 | 210 | 14.10 | 2.53 | 11.5 | 466 |
| 32-64 | 480 | 13.63 | 6.43 | 7.1 | 668 |
| 6-64 | 1850 | 17.25 | 5.13 | 12.0 | 451 |
| 5-64 | 2250 | 12.11 | 2.21 | 9.8 | 528 |
| 7-64 | 2810 | 16.31 | 0.62 | 15.6 | 362 |
| 2-64 | 2970 | 17.03 | -2.10 | 19.0 | 302 |

Clayton and Kieffer, 1991.

**Table 5.** Input data for equation (17) for magnetite and quartz at 1 kb, hydrothermal conditions, and dry conditions for quartz: Linear cooling rate was estimated at 500°C/Ma. Diffusion characteristics ($D_o$, E), A is diffusional anisotropy parameter, a = radius of mineral grain. Temperatures (°C) were calculated for grains with radii of 5 μm for the fine grained outcrops like 35 & 36 and 0.1 cm for coarser grained outcrops nearer to the contact with the Duluth Complex.

| Mineral | $P(H_2O)$ | Reference | dT/dt (°C/Ma) | $D_o$ ($cm^2/s$) | E (J/mol) | A | T (°C); 0.0005 cm | T (°C); 0.1 cm |
|---|---|---|---|---|---|---|---|---|
| magnetite | 1 kb; hydrothermal | Giletti and Hess (1988) | 500 | 3.50E-06 | 188000 | 55 | 383 | 648 |
| magnetite | 1 kb; hydrothermal | Giletti and Hess (1988) | 2050 | 3.50E-06 | 188000 | 55 | 410 | 700 |
| quartz | 1 kb; hydrothermal | Dennis (1984a) | 500 | 2.09E-07 | 138540 | 8.7 | 286 | 561 |
| quartz | 1 kb; hydrothermal | Dennis (1984a) | 2050 | 2.09E-07 | 138540 | 8.7 | 312 | 618 |
| quartz | dry | Sharp et al. (1991) | 500 | 2.10E-08 | 159000 | 8.7 | 415 | 787 |
| quartz | dry | Dennis (1984b) | 500 | 3.00E-07 | 222000 | 8.7 | 288 | 565 |

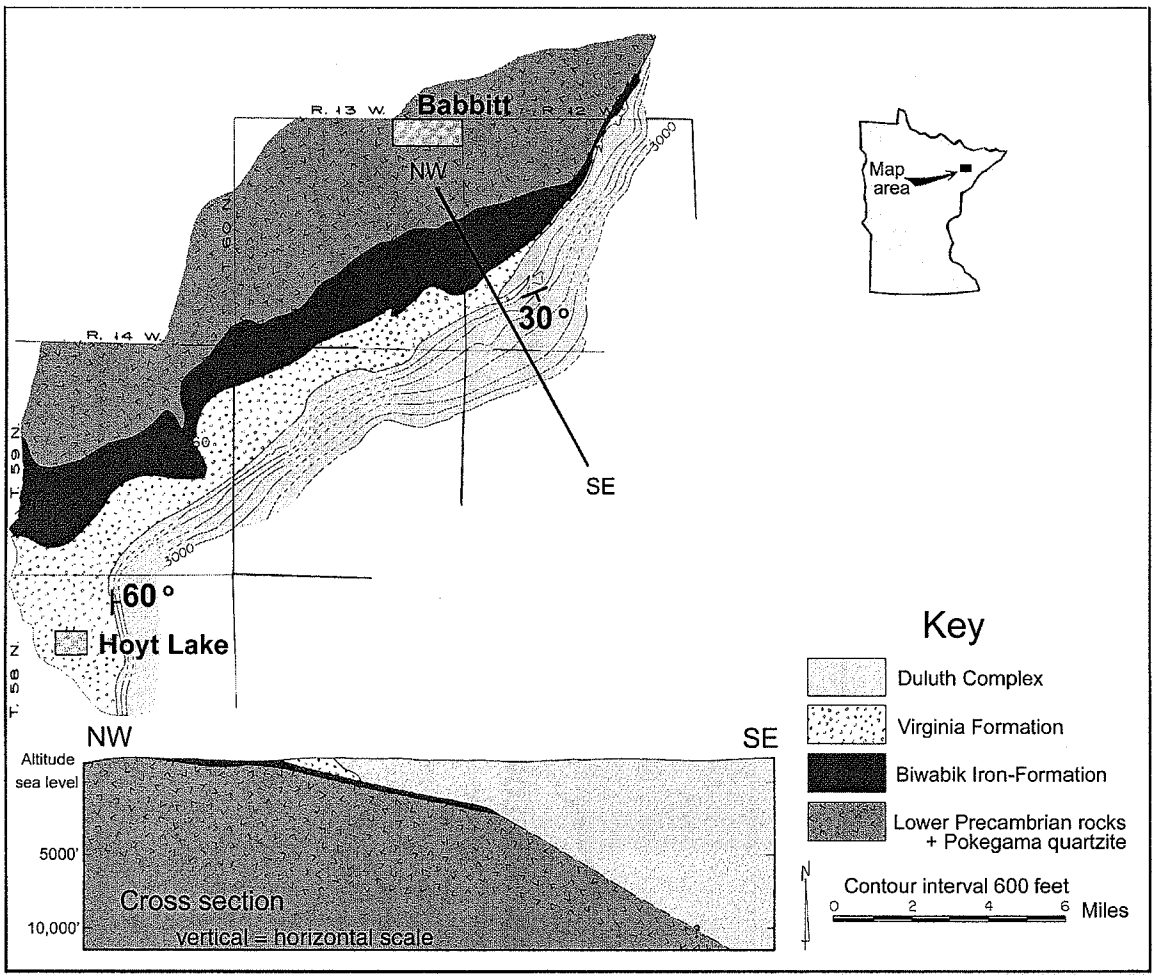


**Figure 1.** Geologic map of the Biwabik Iron-formation and surrounding formations, with average dips of the contact of the Duluth Complex. The cross section shows the stratigraphic relations of the formations. As the Pokegama quartzite is only locally present, it was grouped with the Lower Precambrian rocks. The numbered contours in the Duluth Complex represent depth (ft) to the contact with the country rock. Modified from Bonnichsen, (1972).

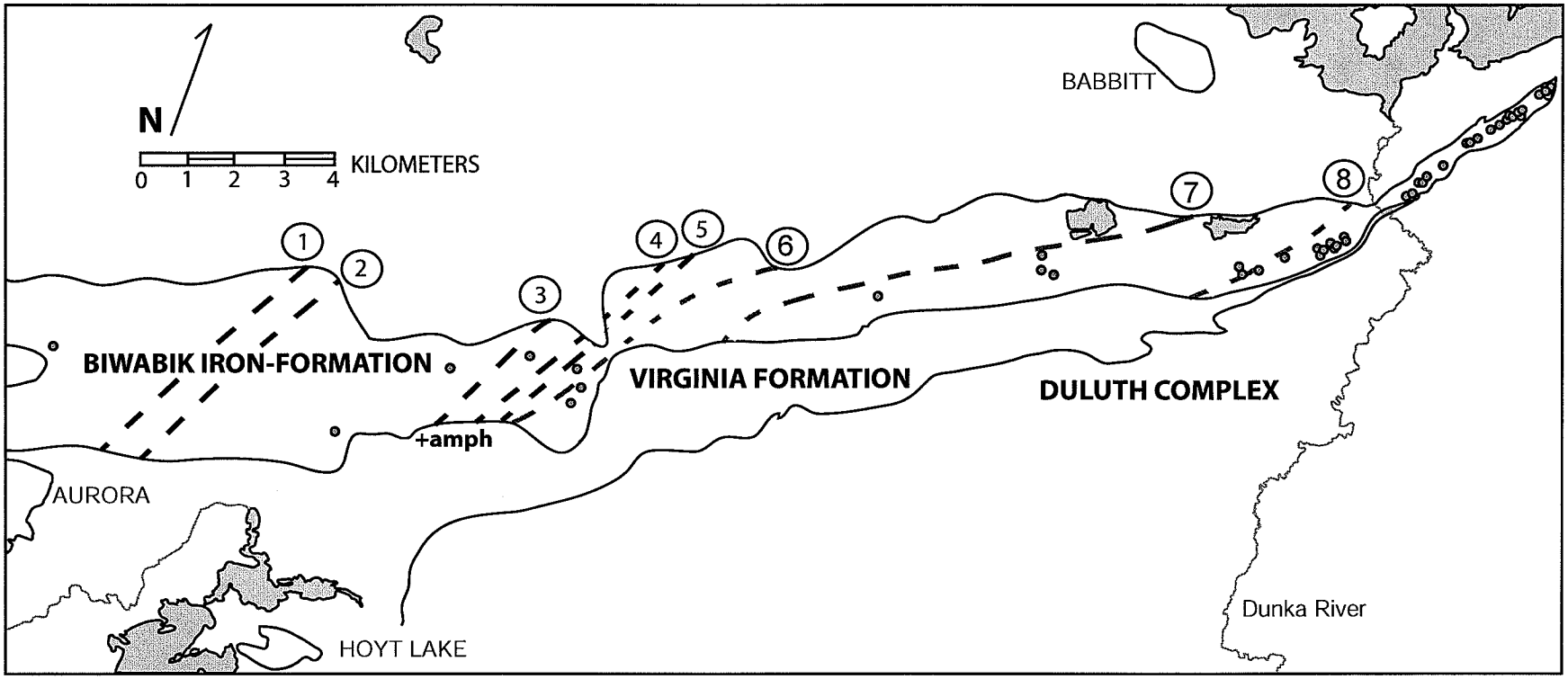


**Figure 2.** Map showing isograds in the Biwabic iron-formation and sample locations. The French (1968) isograds are as follows: 1. partial reduction of hematite to magnetite, 2. formation of clinozoisite, 3. formation of grunerite, 4. formation of hedenbergite and the complete reduction of hematite to magnetite; two close isograds that were condensed to one for the scale of this map, and 5. the formation of ferrohypersthene coupled with graphite. The Frost (2001) isograds are: amphibole isograd (similar to 3), 6. hedenbergite, 7. fayalite, and 8. orthopyroxene.

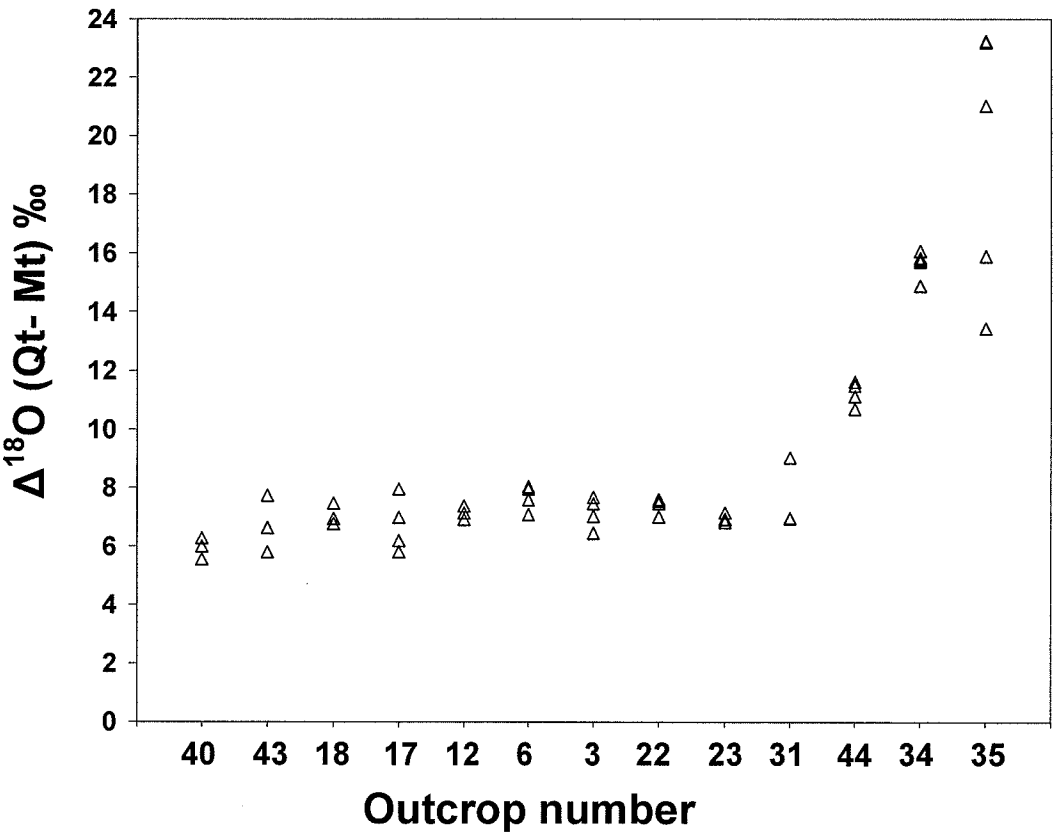


**Figure 3a.** $\Delta^{18}O$ (Qt-Mt) values from outcrops with more than three hand samples, arranged in order of increasing distance from the contact with the Duluth Complex. The standard deviations of the values range from 0.15‰ (±21°C; equation 2), outcrop 22 (UW1962.22) to 5.53‰ (±82°C; equation 2), outcrop 35 (UW1962.35).

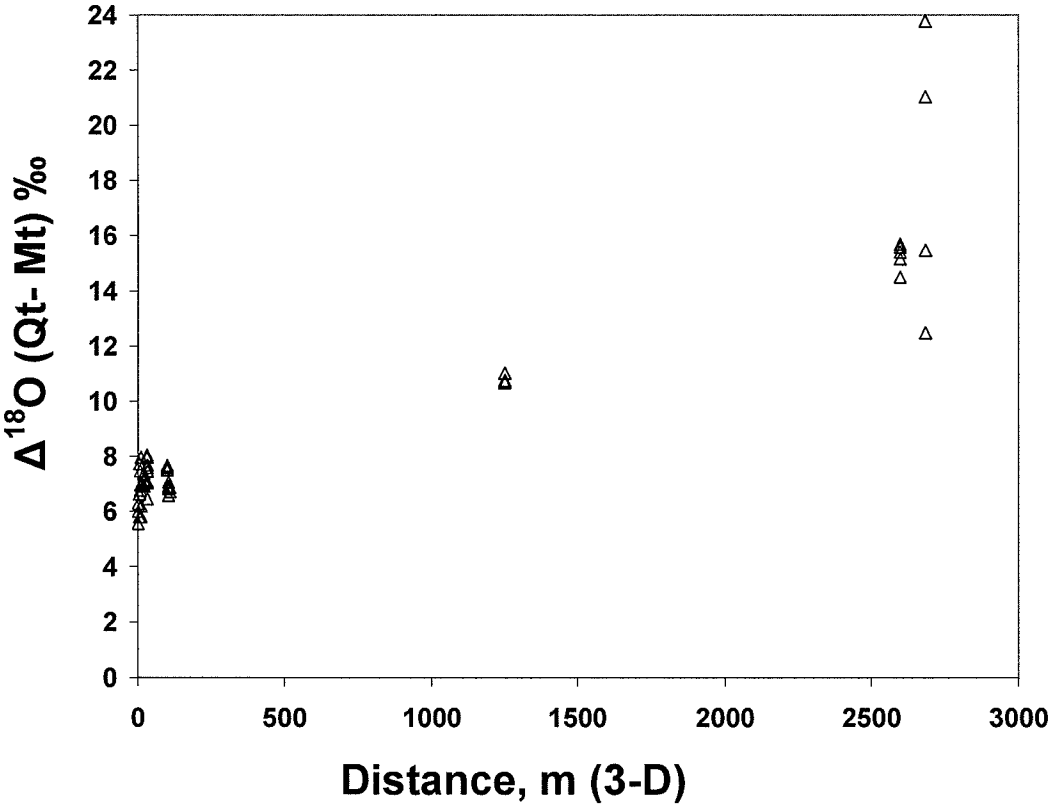


**Figure 3b.** Distance from the contact (3-D) with the Duluth Complex vs. $\Delta^{18}O$ (Qt-Mt) values from outcrops with more than three hand samples (numbered in 3a) to show relationship over distance. The standard deviations of the values increase from 0.15‰ (±21°C; equation 2), outcrop 22 (UW1962.22) to 5.35‰ (±82°C; equation 2), outcrop 35 (UW1962.35).

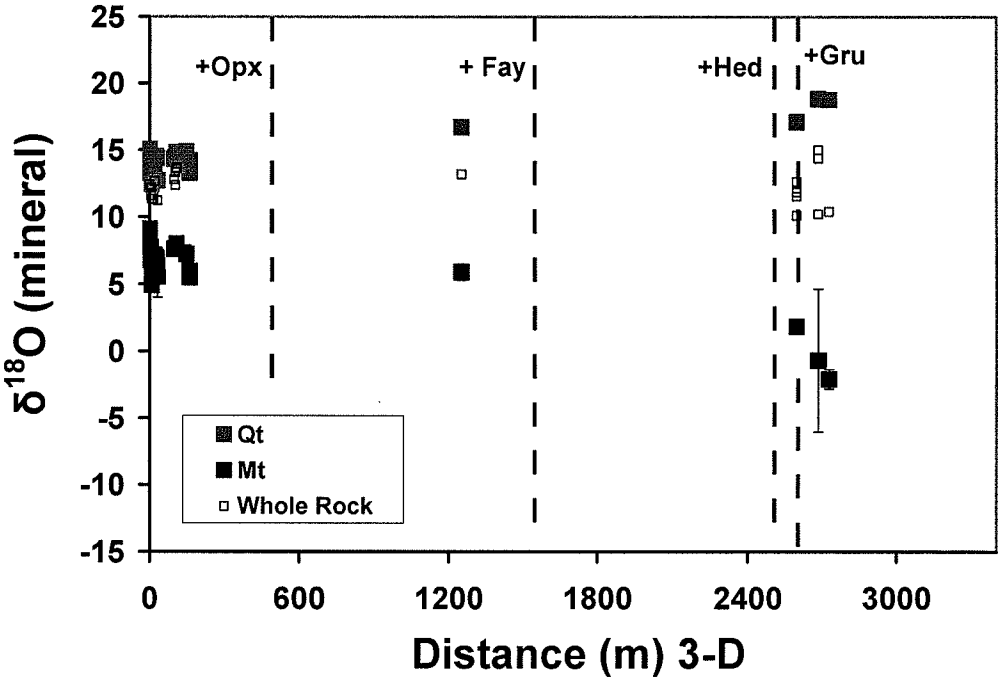


**Figure 4.** Graph of $\delta^{18}O$ vs. distance (3-D) to the contact with the Duluth Complex. Note that the change of quartz values is less than the change of magnetite values. Also note that fractionations decrease and temperatures increase towards the contact with the Duluth Complex. Whole rock values are relatively constant, 12.48 ±0.87‰ for samples less than 0.2 km from the contact and 12.38 ±2.01‰ for samples greater than 2.5 km from the contact. Uncertainty is one standard deviation of the values for each outcrop. The analytical uncertainty is less than the size of the dots. Approximate locations of the isograds: formation of grunerite, hedenbergite, fayalite and orthopyroxene, are shown.

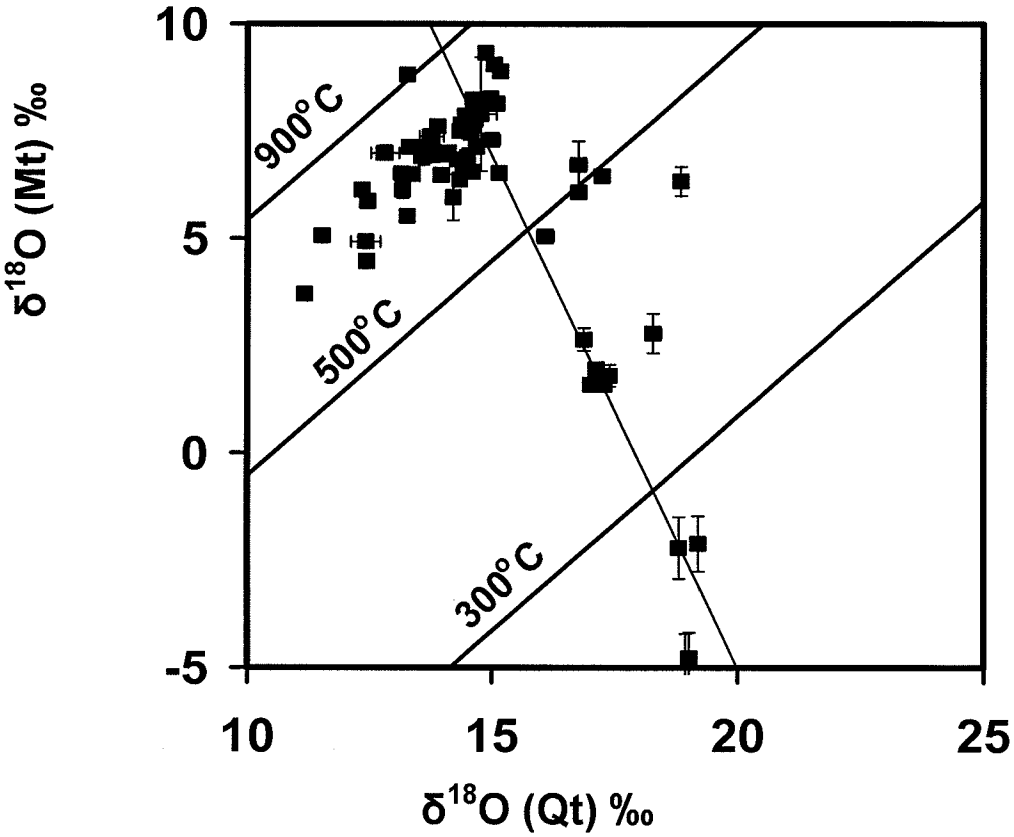


**Figure 5.** Plot of $\delta^{18}O$ (quartz) vs. $\delta^{18}O$ (magnetite) with equilibrium temperatures. The uncertainty shown is one standard deviation of the hand samples. The analytical uncertainty is less than the size of the dots. The line with a negative slope of ~3/1 is a visual fit through the data showing the relative modal percentages of quartz and magnetite which are ~75% quartz and ~25% magnetite. Because of this oxygen ratio and the mass balance in the $\delta^{18}O$ (whole rock) values (Table 3), magnetite $\delta^{18}O$ values change more with temperature than quartz.

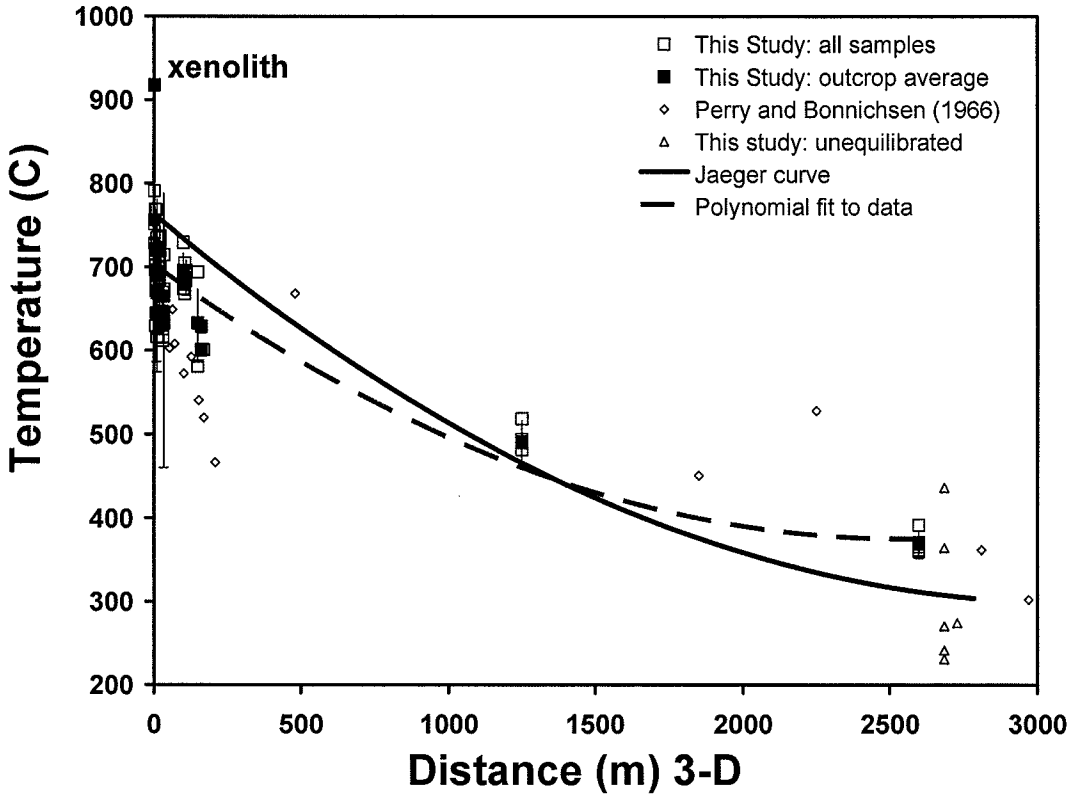


**Figure 6a.** A graph of distance (3-D) from the contact with the Duluth Complex vs. the average outcrop temperature. The uncertainty in the temperature is based on the standard deviation of the hand sample $\Delta^{18}O$ (Qt-Mt) values for each outcrop. Perry and Bonnichsen's (1966) samples are lower in temperature closest to the contact than this study. The solid curve is the predicted thermal profile (equations 21-22; Jaeger, 1959) (see text). The dashed curve is a second order polynomial fit through the data and is concave up which is consistent with the cooling of a simple tabular intrusive body (Jaeger, 1957) and small amounts of fluid flow.

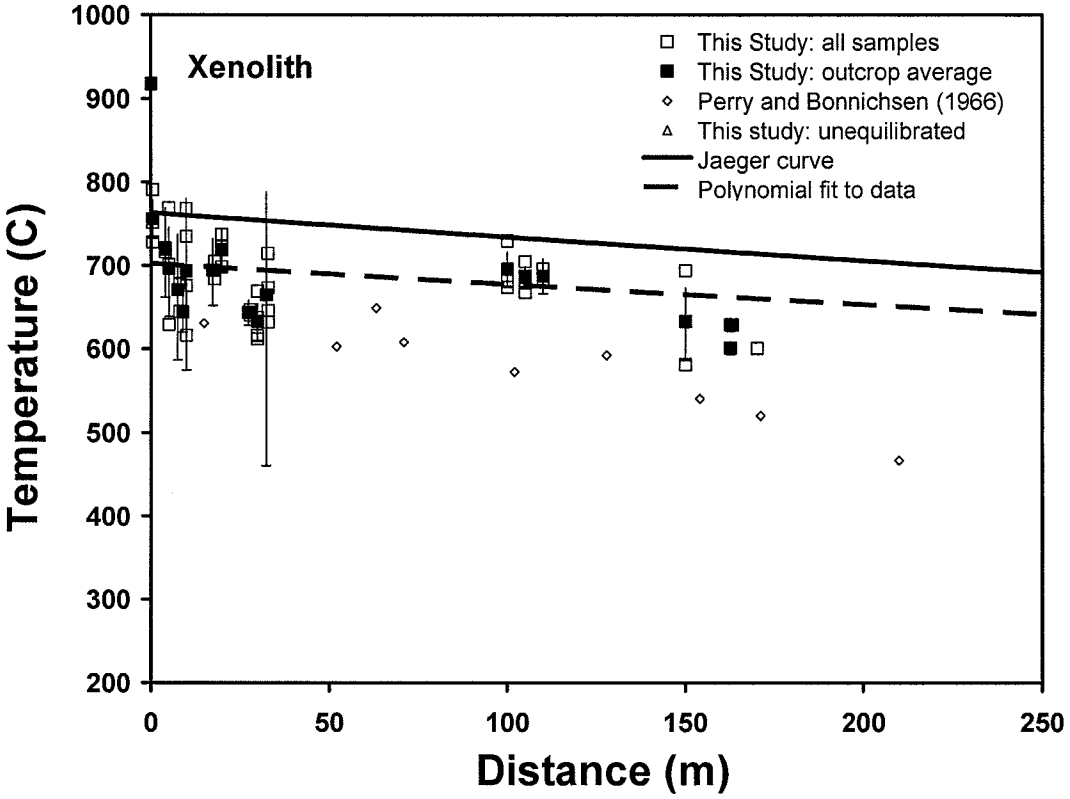


**Figure 6b.** A graph of distance from the contact (3-D) with the Duluth Complex vs. the average outcrop temperature showing only the samples less than 250 m from the contact. The uncertainty in the temperature is based on one standard deviations of the hand sample $\Delta^{18}O$ (Qt-Mt) values for each outcrop.

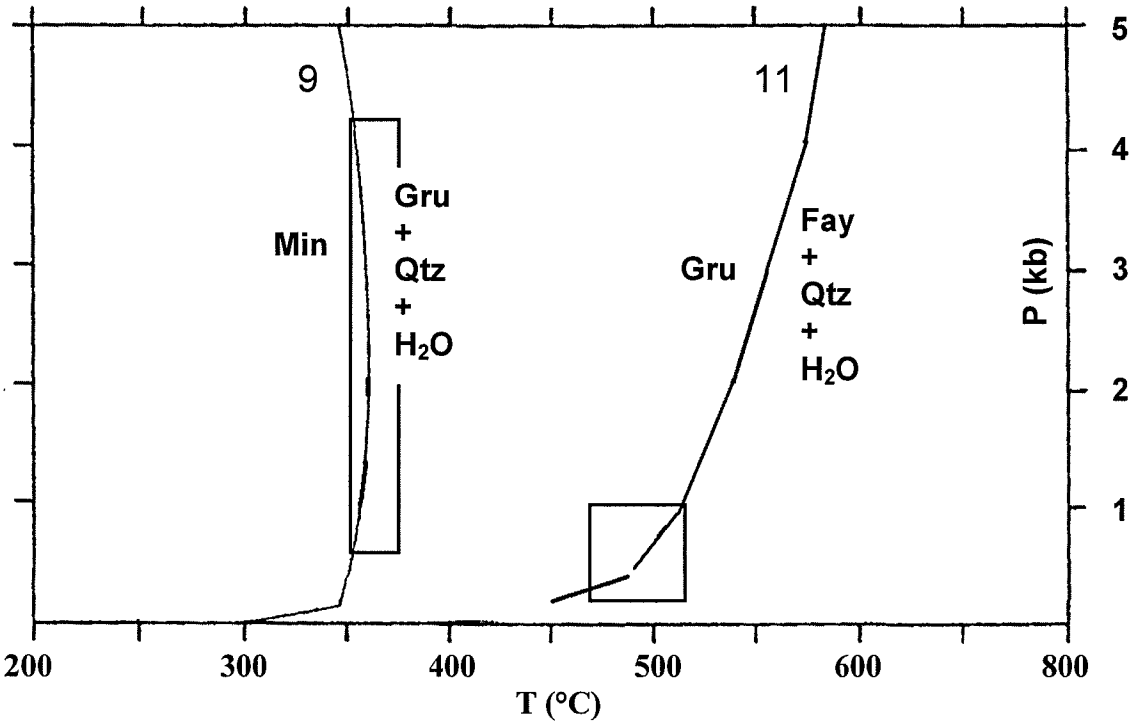


**Figure 7.** Dehydration reactions in the quartz saturated portion of the system $FeO\text{-}SiO_2\text{-}H_2O$. Reaction (12) from Jenkins and Bozhilov (2003), reaction (9) from Evans and Guggenheim (1988). Qtz = quartz, Min = minnesotaite, Gru = grunerite, and Fay = fayalite. The boxes are centered over the average temperature and the width is ± one standard deviation.

## REFERENCES CITED

Andrews, M.S., and Ripley, E.M., 1987, Contact metamorphism of the Virginia formation at the Dunka road deposit, Minnesota, Geological Society of America Abstracts with Programs, v.19; 4, p. 186-187.

Becker, R.H. and Clayton, R.N., 1976, Oxygen isotope study of a Precambrian banded iron-formation, Hamersley Range, Western Australia, Geochimica et Cosmochimica Acta, v. 40, p. 1153-1165.

Bohlen, S.R., and Boettcher, A.L., 1981, Experimental investigations and geological applications of orthopyroxene geobarometry, American Mineralogist, v. 66, p. 951-964.

Bohlen, S.R., and Essene, E.J., 1977, Feldspar and oxide thermometry of granulites in the Adirondack Highlands, Contributions to Mineralogy and Petrology, v. 62; 2, p. 153-169.

Bonnichsen, B., 1969, Metamorphic pyroxenes and amphiboles in the Biwabik iron formation, Dunka River area, Minnesota, Mineralogical Society of America, special paper 2, p. 217-239.

Bonnichsen, B., 1972, Southern part of the Duluth Complex, Geology of Minnesota: a Centennial Volume, Sims, P.K. and Morey, G.B., eds., p. 361-388.

Bonnichsen, B., 1975, Geology of the Biwabik Iron Formation, Dunka River Area, Minnesota, Economic Geology, v. 70, p. 319-340.

Bowers, T.S. and Taylor, H.P., 1985, An integrated chemical and stable-isotope model of the origin of Midocean Ridge hot spring systems, Journal of Geophysical Research, v. 90; no. B14, p. 12583-12606.

Brandriss, M.E., O'Neil, J.R., Edlund, M.B., and Stoermer, E.F., 1998, Oxygen isotope fractionation between diatomaceous silica and water, Geochimica et Cosmochimica Acta, v. 62; 7, p. 1119-1125.

Buddington, A.F., and Lindsley, D.H., 1964, Iron-titanium oxide minerals and synthetic equivalents, Journal of Petrology, v. 5, p. 310-357.

Clayton, R.N., and Kieffer, S.W., 1991, Oxygen isotopic thermometer calibrations, The Geochemical Society Special Publication, Taylor, H.P., O'Neil, J.R., and Kaplan, I.R., eds., v. 3, p. 3-10.

Dennis, P.F., 1984a, Oxygen self diffusion in quartz under hydrothermal conditions, Journal of Geophysical Research, v. 89, p. 4047-4057.

Dennis, P.F., 1984b, Oxygen self diffusion in quartz, Progress in Experimental Petrology, v. 6, p. 260-265.

Dodson, M.H., 1973, Closure temperature in cooling ages, Contributions to Mineralogy and Petrology, v. 40, p. 259-274.

Evans, B.W. and Guggenheim, S., 1988, Talc, pyrophyllite, and related minerals, Mineralogical Society of America Reviews in Mineralogy, Bailey, S.W., ed., v. 19, p. 225-294.

Floran, R.J., and Papike, J.J., Mineralogy and petrology of the Gunflint Iron Formation, Minnesota-Ontario: correlation of compositional and assemblage variations at low to moderate grade, Journal of Petrology, v. 19; 2, p. 215-288.

Fortier, S.M., and Giletti, B.J., 1989, An empirical model for predicting diffusion coefficients in silicate minerals, Science, v. 245; 4925, p. 1481-1484.

French, B.M., 1968, Progressive contact metamorphism of the Biwabik Iron Formation, Mesabi Range, Minnesota, Minnesota Geological Survey Bulletin, v. 45, p.1-103.

French, B.M., 1973, Mineral assemblages in diagenetic and low-grade metamorphic iron-formation, Economic Geology, v. 68, p. 1063-1074.

Frost, 2001, personal communication.

Giletti, B.J., and Hess, K.C., 1988, Oxygen diffusion in magnetite, Earth and Planetary Science Letters, v. 89, p. 115-122.

Gregory, R.T. and Taylor, H.P., Jr., 1981, An oxygen isotope profile in a section of Cretaceous oceanic crust, Samail Ophiolite, Oman: evidence for $\delta\ ^{18}O$ buffering of the oceans by deep (>5 km) seawater-hydrothermal circulation at Mid-Ocean Ridges, Journal of Geophysical Research, v. 86; B4, p. 2737-2755.

Gregory, R.T., Criss, R.E., and Taylor, H.P., 1989, Oxygen isotope exchange kinetics of mineral pairs in closed and open systems: applications to problems of hydrothermal alteration of igneous rocks and Precambrian iron formations, Chemical Geology, v. 75; 1-2, p. 1-42.

Gundersen, J.N., and Schwartz, G.M., 1962, The geology of the metamorphosed Biwabik Iron Formation, Eastern Mesabi district, Minnesota, Minnesota Geological Survey Bulletin, v. 43, p. 1-139.

Hauck, S.A., Severson, M.J., Zanko, L., Barnes, S.J., Morton, P., Alminas, H., Foord, E.E., and Dahlberg, E.H., 1997, An overview of the geology and oxide, sulfide,

and platinum-group element mineralization along the western and northern contacts of the Duluth Complex, Geological Society of America Special Paper 312, p. 137-185.

Jaeger, J.C., 1957, The temperature in the neighborhood of a cooling intrusive sheet, American Journal of Science, v. 255, p. 306-318.

Jaeger, J.C., 1959, Temperatures outside a cooling intrusive sheet, American Journal of Science, v. 257, p. 44-54.

Jenkins, D.M. and Bozhilov, K.N., 2003, Stability and thermodynamic properties of ferro-actinolite: a re-investigation, American Journal of Science, v. 303, p. 723-752.

Knauth, L.P., 1998, Salinity, temperature, and oxygen history of the Precambrian ocean, Abstracts with Programs, Geological Society of America, v. 30; 7, p. 272.

Knauth, L.P., and Epstein, S., 1976, Hydrogen and oxygen isotope ratios in nodular and bedded cherts, Geochimica et Cosmochimica, v. 40, p. 1095-1108.

Knauth, L.P. and Lowe, D.R., 2003, High Archean climatic temperature inferred from oxygen isotope geochemistry of cherts in the 3.5 Ga Swaziland Supergroup, South Africa, Geological Society of America Bulletin, v. 115, 5; p. 566-580.

Koptev-Dornikov, E.V., Chalokwu, C.I., Arskin, A.A., and Grant, N.K., 1995, Forward modeling of incompatible element enrichment in the basal zone of the Partridge River intrusion, Eos, Transactions, American Geophysical Union, v. 76 supplement, p. 288.

Lindsley, D.H., 1983, Pyroxene thermometry, American Mineralogist, v. 68, p. 477-493.

Mandernack, K.W., Bazylinski, D.A., Shanks III, W.C., and Bullen, T.D., 1999, Oxygen and iron isotope studies of magnetite produced by magnetotactic bacteria, Science, v. 285, p. 1892-1896.

Miller, J.D., 1999, Discovery of stratiform PGE mineralization in tholeiitic layered intrusions, northeastern Minnesota, Abstracts with Programs, Geological Society of America, v. 31; 7, p. 32-33.

Miyano, T. and Klein, C., 1986, Fluid behavior and phase relations in the system Fe-Mg-Si-C-O-H: Application to high grade metamorphism of iron-formations, American Journal of Science, v. 286, p. 540-575.

Morey, G.B., 1972, Mesabi Range, Geology of Minnesota, Minnesota Geological Survey Centennial Volume, Sims, P.K. and Morey, G.B., eds., p. 204-217.

Morey, G.B., 1983, Animikie Basin, Lake Superior Region, USA, Iron-Formation: Facts and Problems, Trendall, A.F. and Morris, R.C., eds., p. 13-67.

Morey, G.B., Papike, J.J., Smith, R.W., and Weiblen, P.W., 1972, Observations on the contact metamorphism of the Biwabik iron-formation, east Mesabi district, Minnesota, Geological Society of America Memoir 135, p. 225-263.

Muehlenbachs, K., 1986, Alteration of the oceanic crust and the $^{18}O$ history of seawater, Mineralogical Society of America Reviews in Mineralogy, Valley, J.W., Taylor, H.P., and O'Neil, J.R., eds., v. 16, p. 425-444.

Muehlenbachs, K., 1998, Errors on the estimate of the oxygen isotope ratio of ancient seawater, Geological Society of America Abstracts with Programs, v. 30; 7, p. 272.

Muehlenbachs, K., 2001, Ophiolites as faithful records of the oxygen isotope ratio of ancient seawater, Geological Society of America Abstracts with Programs, v. 33; 6, p. 225.

Muehlenbachs, K., and Clayton, R.N., 1976, Oxygen isotope composition of the oceanic crust and its bearing on seawater, Journal of Geophysical Research, v. 81; 23, p. 4365-4369.

Perry, E.C., 1967, The Oxygen isotope chemistry of ancient cherts, Earth Planetary Science Letters, v. 3; 62-66, p. 176-179.

Perry, E.C. and Ahmad, S.N., 1983, Oxygen isotope geochemistry of Proterozoic chemical sediments, Geological Society of America Memoir 161, p. 253-263.

Perry, E.C., and Bonnichsen, B., 1966, Quartz and magnetite: oxygen 18-oxygen 16 fractionation in metamorphosed Biwabik formation, Science, v. 153, p. 528-529.

Perry, E.C. and Lefticariu, L., 2003, Formation and geochemistry of Precambrian cherts, Treatise on Geochemistry, Holland, H., and Turekian, K., eds., v. 7, p. 99-113.

Perry, E.C. and Tan, F.C., 1972, Significance of oxygen and carbon isotope variations in early Precambrian cherts and carbonate rocks of Southern Africa, Geological Society of America Bulletin, v. 83; 3, p. 647-664.

Perry, E.C., Tan, F.C., and Morey, G.B., 1973, Geology and stable isotope chemistry of the Biwabik Iron Formation, northern Minnesota, Economic Geology, v. 68, p. 1110-1125.

Ripley, E.M. and Alawi, J.A., 1988, Petrogenesis of politic xenoliths at Babbitt Cu-Ni

deposit, Duluth Complex, Minnesota, U.S.A., Lithos, v.21; 2, p. 143-159.

Ripley, E.M., Park, Y.R., Lambert, D.D., and Frick, L.R., 2001, Re-Os variations in carbonaceous pelites hosting the Duluth Complex, implications for metamorphic and metasomatic processes, Geochimica et Cosmochimica Acta, v. 65; 17, p. 2965-2978.

Robert, F., Rejou-Michel, A., and Javoy, M., 1992, Oxygen isotopic homogeneity of the Earth: new evidence, Earth and Planetary Science Letters, v. 108, p. 1-9.

Sharp, Z.D., Giletti, B.J., and Yoder, H.S., 1991, Oxygen diffusion rates in quartz exchanged with $CO_2$, Earth and Planetary Science Letters, v. 107, p.339-348.

Simmons, E.C., Lindsley, D.H., and Papike, J.J., 1974, Phase relations and crystallization sequence in contact-metamorphosed rock from the Gunflint Iron Formation, Minnesota, Journal of Petrology, v. 15, p. 539-565.

Sims, P.K., and Viswanathan, S., 1972, Giants Range Batholith, The Geology of Minnesota- a Centennial Volume, Sims, P.K. and Morey, G.B., eds., p. 120-139.

Spicuzza, M.J., Valley, J.W., Kohn, M.J., Girard, J.P., and Fouillac, A.M., 1998, The rapid heating, defocused beam technique; a $CO_2$ laser-based method for highly precise and accurate determination of $\delta^{18}$ O values of quartz, Chemical Geology, v. 144; 3-4, p. 195-203.

Tuttle, O.F., and Bowen, N.L., 1958, Origin of granite in light of experimental studies in the system $NaAlSi_3O_8$-$KAlSi_3O_8$-$SiO_2$-$H_2O$, Geological Society of America Memoir, v. 74, p. 1-153.

Valley, J.W., 2001, Stable isotope thermometry at high temperatures, Mineralogical Society of America Reviews in Mineralogy and Geochemistry, Valley, J.W., and Cole, D.R., eds., v. 43, p. 365-413.

Valley, J.W., Kitchen, N., Kohn, M., Niendorf, C.R., and Spicuzza, M.J., 1995, UWG-2, a garnet standard for oxygen isotope ratios: strategies for high precision and accuracy with laser heating, Geochimica et Cosmochimica Acta, v. 59; 24, p. 5223-5231.

Veizer, J., 1997, Phanerozoic Seawater: New oxygen, carbon and strontium isotope databases, EOS Transactions v. 78; 46, pp. 829-830.

Veizer, J. and Hoefs, J., 1976, The nature of $O^{18}/^{16}O$ and $C^{13}/C^{12}$ secular trends in sedimentary carbonate rocks, Geochemica et Cosmochemica Acta, v. 40, p. 1387-1395.

Weiblen, P.W., and Morey, G.B., 1980, A summary of the stratigraphy, petrology and structure of the Duluth Complex, American Journal of Science, v. 280, p. 88-133.

Winhusen E., 2000, Precambrian seawater paleotemperature analysis using oxygen isotopes from Hamersley carbonates, Australia, Abstracts with Programs, Geological Society of America, v. 32; 4, p. 68.

Winter, B.L. and Knauth, L.P., 1992, Stable isotope geochemistry of cherts and carbonates from the 2.0 Ga Gunflint Iron Formation; implications for the depositional setting, and effects of diagenesis and metamorphism, Precambrian Research, v. 59, p. 283-313.

Zheng, Y.F., and Fu, B., 1998, Estimation of oxygen diffusivity from anion porosity in minerals, Geochemical Journal, v. 32, p. 71-89.

## APPENDIX 1.

## BANDED IRON-FORMATION

BIFs range from 3.8 - 0.7 Ga in age with peak rates of deposition between 2.4-2.3 Ga (Fig. A1, Isley, 1995). While the age of at least one of the iron-formations has changed, this gives a general idea of production through time. The formation of BIF is related to higher concentrations of iron in the Archean and Proterozoic oceans (Frei et al., 1999) than today allowing for such large quantities of iron precipitation from the seawater as hematite or magnetite, intercalated with chert. The deposition of BIF is thought to be associated with increased production of $O_2$ by photosynthesis that led to the creation of a stable oxygenated atmosphere about 2.0 Ga (Brown et al., 1995; Frei et al., 1999; Farquhar et al., 2001). Mechanism aside, there is convincing evidence for a step increase in the $O_2$ content in the atmosphere between 2.25 and 2.06 Ga (Holland, 1994). Studies of paleosols show that the P ($O_2$) was $\leq$ 1% present atmospheric levels (PAL), and has been $\geq$ 15% PAL since 1.9 Ga, as indicated by the behavior of iron during soil formation. However, other work has led some to suggest this rise in P ($O_2$) may have been before 2.2-2.3 Ga (Marmo and Ohmoto, 2000; Ono and Ohmoto, 2000).

Banded iron-formations may have a complex history of diagenesis, metamorphism, and uplift (e.g. Perry et al., 1973; Bonnichsen, 1975; Morey, 1999). However, due to the prevalence of BIFs in shield terranes worldwide: in North and South America, Greenland, Asia, Australia, and Africa, they are an important source of information on the Earth's history during the Archean and Proterozoic (e.g. Goodwin, 1973; Perry et al., 1973; Bonnichsen, 1975; Lougheed, 1983; Horstmann et al., 1995; Baio et al., 1996; Frei et al., 1999; Klein et al. 2002). A key part of the Earth's history is the beginning of life and BIFs

have some of the earliest evidence of life from the Archean Isua formation of Western Greenland that has $\delta^{13}C$ values consistent with a biogenic origin (Schidlowski, 2001). However, Van Zuilen et al., 2002, suggest caution for interpreting ancient life from $\delta^{13}C$ values, as previously classified sedimentary carbon and the basis of the interpretation of $\delta^{13}C$ from the Isua Supercrustal Belt as ancient traces of life are now thought by some to have been a result of metasomatism.

BIFs are important for other reasons. Economically, BIFs are the source of billions of metric tons of iron ore (Isley, 1995; Klein et al. 2002). Ninety percent of iron extracted globally comes from mining BIFs, thus they are important natural resource (Isley, 1995).

There are different ways to name the types of BIF. One is to categorize them based on the characteristics of their depositional basins and associated rocks (Gross, 1979), with names based on the type locality. The two dominant types are the Lake Superior-type and Algoma-type BIFs. The Lake Superior-type was deposited with quartzite, dolomite, and black shale in continental shelf environments. The Algoma type is associated with volcanic and greywacke rock assemblages along volcanic arcs, rift zones and deep-seated fault fracture systems (Gross, 1979; Johnson et al., 2003). Another categorization is to name them based on sedimentary facies as determined by their mineralogy (James, 1954), with four intergradational facies: oxide, silicate, carbonate, and sulfide. The oxide facies iron minerals are dominated by hematite and magnetite. In the carbonate facies the carbonate is dominated by siderite and the carbonate facies is mostly deposited in deep water. The silicate facies has primary iron silicate minerals. The sulfide facies has disseminated pyrite in black shale, or pyrite and pyrrhotite mixed with siderite and carbonate ± banded chert or quartz (Goodwin, 1973). The sulfide facies is the least common, and it is often thin and discontinuous.

***Formation of BIF***

Theories conflict as to how the BIFs were deposited. Some workers think BIFs were chemically formed as an oxide-carbonate rock (Mackenzie and Gees, 1971; Manikyamba et al., 1994; Frei et al., 1999). Therefore, the present texture of the BIFs is correlative to depositional environment: coarse cherty BIFs are thought to have formed in shallow water, high energy environments; and slaty BIFs are believed to have formed in deep water, low energy environments (Perry et al., 1973; Lougheed et al., 1983; Manikyamba et al., 1994). This means iron concentrations in Archean seawater were locally high, related to hydrothermal flux of water through oceanic ridges and other hydrothermal systems, (Fig. A2), before more oxidizing conditions evolved at the end of the Paleoproterozoic (Isley, 1995; Frei et al., 1999). In contrast, Brown et al., 1995, argue that the accumulation of iron and silica in BIFs cannot be explained by inorganic chemical processes only, and that the deposition of BIFs involved microbially-mediated geochemical processes. To support this hypothesis, they cite recent studies on biofilms that sorb silica and precipitates iron as siderite and hematite (Brown et al., 1995). While they do not conclude a direct role of bacteria in BIF genesis, the $\delta^{56}$ Fe study of Johnson et al. (2003) suggests that $\delta^{56}$ Fe values of 0 to +1‰ found in Late Archean to Early Proterozoic BIFs may be explained by photosynthetic oxidation of Mid-Oceanic Ridge (MOR) Fe (II) sources.

There is also a competing theory that the magnetite, quartz and sulfides in BIFs formed post-depositionally. Lougheed (1983) advocates that BIFs were deposited originally as carbonates, and that the formation of hematite and magnetite resulted from later oxidation of siderite. This was followed by silicification to form BIFs. Textural evidence such as

magnetite pseudomorphs after gypsum and quartz grains containing ghost structures that are believed to be relicts of cleavage or twinning of the original sparry calcite support this theory (Lougheed, 1983). But other textural investigations into BIFs support that the hematite and magnetite are primary (e.g. Perry, 2003; Hoffman et al., 1981; Morey, 1975).

### *BIF Mineralogy*

BIFs are thought to have formed on continental shelves (Fig. 2A; e.g. Perry et al., 1973; Bonnichsen, 1975; Lougheed et al. 1983; Manikyamba et al., 1994). Superior type BIF that has experienced little or no metamorphism is mainly composed of quartz (chert) and magnetite with varying amounts of hematite, siderite, ankerite, greenalite, carbonate, goethite, and pyrite (e.g. Perry and Bonnichsen, 1966; Bonnichsen, 1975; Horstmann et al., 1995; Klein et al., 2002). In metamorphic BIFs along with magnetite and quartz, iron silicates such as orthopyroxene, clinopyroxene, fayalite, minnesotaite, and stilpnomelane, are common with amphiboles, mainly grunerite and cummingtonite, less common (Perry and Bonnichsen, 1966; Bonnichsen, 1975; Klein et al., 2002).

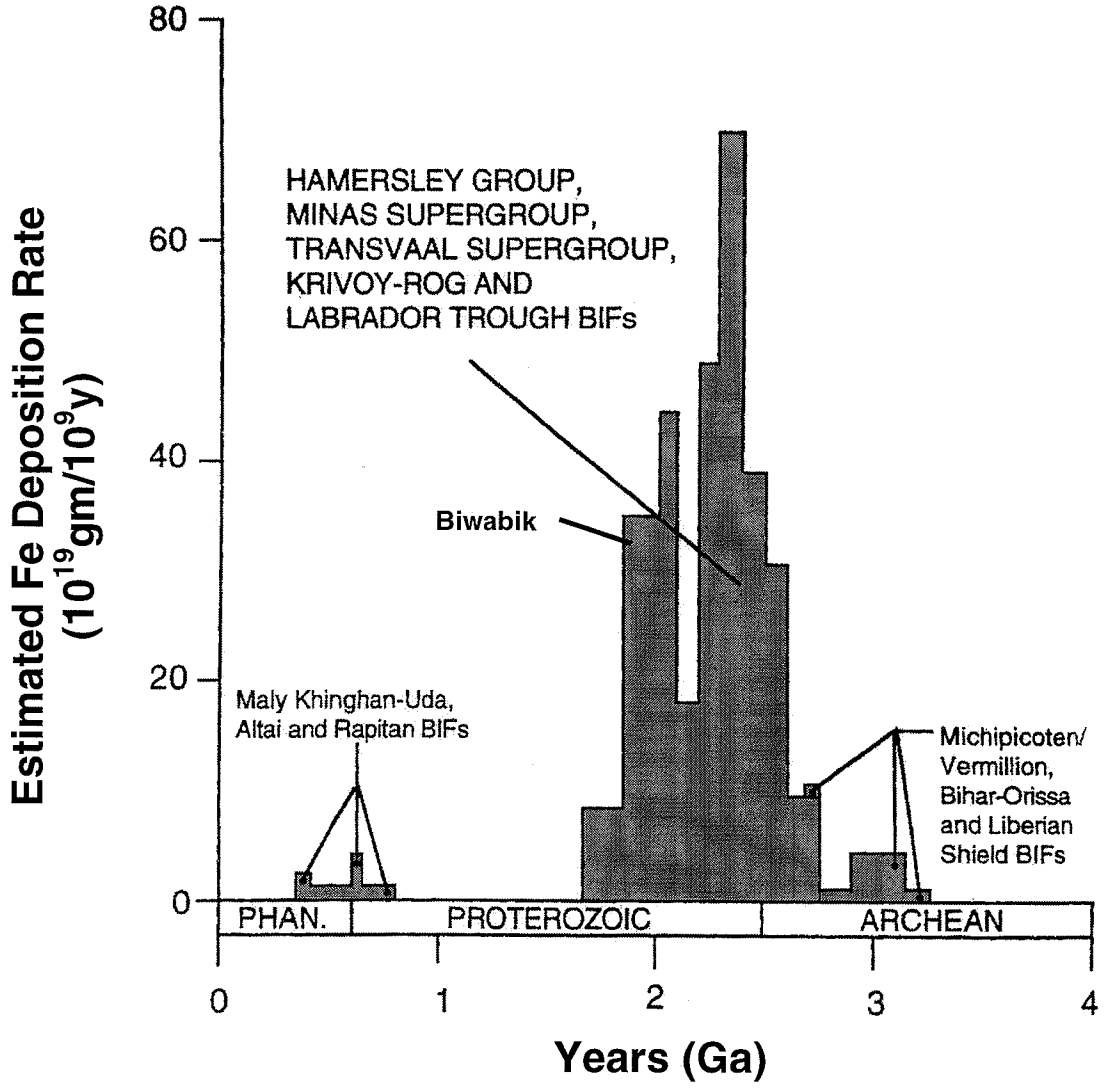


**Figure A1.** Graph of estimated deposition rates ($10^{19}$gm/$10^{9}$y); modified from Isley et al., 1995. Note peak at 2.3-2.4 Ga.

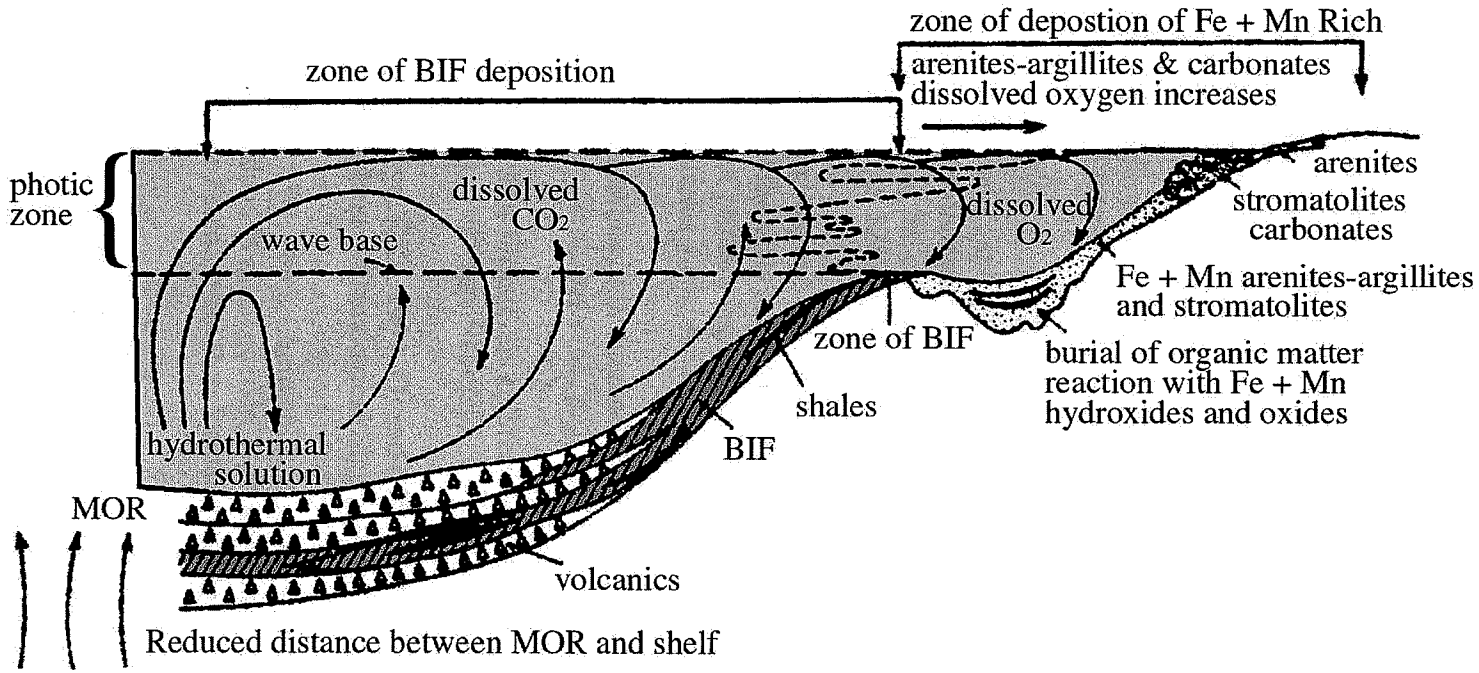


**Figure A2.** Modified from Manikyamba et al., 1999, showing the shelf deposition of BIF with the hydrothermal model with the Mid Oceanic Ridge (MOR) as the source of the hydrothermal solution. The intercalation of BIF and volcanics is typical for Algoma type BIF.

**REFERENCES CITED**

Biao, S., Nutman, A.P., Lui, D., Jiashan, W., 1996, 3800 to 2500 Ma crustal evolution in the Anshan area of Liaoning Province, northeastern China, Precambrian Research, v. 78, p.79-94.

Bonnichsen, B., 1972, Southern Part of the Duluth Complex, Geology of Minnesota: a Centennial Volume, Sims, P.K. and Morey, G.B., eds., p. 361-388.

Bonnichsen, B., 1975, Geology of the Biwabik Iron Formation, Dunka River area, Minnesota, Economic Geology, v. 70, p. 319-340.

Brown, D.A., Gross, G.A., and Sawicki, J.A., 1995, A review of the microbial geochemistry of Banded Iron-Formations, The Canadian Mineralogist, v. 33, p. 1321-1333.

Farquhar, J., Saverino, J., Airieau, S., and Thiemens, M.H., 2001, Observation of wavelength-sensitive mass-independent sulfur isotope effects during $SO_2$ photolysis; implications for the early atmosphere, Journal of Geophysical Research Earth Planets, v. 106; 12, p. 32829-32839.

Frei, R., Bridgewater, D., Rosing, M., and Stecher, O., 1999, Controversial Pb-Pb and Sm-Nd isotope results in the early Archean Isua (West Greenland) oxide iron formation; preservation of primary signatures versus secondary disturbances, Geochimica et Cosmochimica Acta, v. 63, p. 473-488.

French, B.M., 1973, Mineral assemblages in diagenetic and low-grade metamorphic iron-formation, Economic Geology, v. 68, p. 1063-1074.

Goodwin, A.M., 1973, Archean iron-formations and tectonic basins of the Canadian Shield, Economic Geology, v. 68, p. 915-933.

Holland, H.D., Kuo, P.H., and Rye, R.O., 1994, $O_2$ and $CO_2$ in the Late Archean and Early Proterozoic atmosphere, Mineralogical Magazine, v. 58A, p. 424-425.

Horstmann, U.E., and Halbich, I.W., 1995, Chemical composition of banded iron-formations of the Griqualand West Sequence, Northern Cape Province, South Africa, in comparison with other Precambrian iron formations. Precambrian Research, v. 72, p. 109-145.

Insley, A.E., 1995, Hydrothermal plumes and the delivery of iron to banded iron formation, Journal of Geology, v. 103, p. 169-185.

Johnson, C.M., Beard, B.L., Beukes, N.J., Klein, C., and O'Leary, J.M., 2003, Ancient

geochemical cycling in the Earth as inferred from Fe isotope studies of banded iron formations from the Transvaal Craton, Contributions to Mineralogy and Petrology, v. 144, p. 523-547.

Klein, C. Ladeira, E., 2002, Petrography and geochemistry of the least altered banded iron-formation of the Archean Carajas formation, northern Brazil, Economic Geology, v. 97, p. 643-651.

Lougheed, M.S., 1983, Origin of Precambrian iron-formations in the Lake Superior region, Geological Society of America Bulletin, v. 94, p. 325-340.

Mackenzie, F.T. and Gees, R., 1971, Quartz: synthesis at Earth-surface conditions, Science, v. 173, p. 515-535.

Manikyamba, C., and Naqvi, S.M., 1995, Geochemistry of Fe-Mn formations of the Archaean Sandur schist belt, India – mixing of clastic and chemical processes at a shallow shelf, Precambrian Research, v. 72, p. 69-95.

Marmo, J.S. and Ohmoto, H., 2000, ~2.3 Ga Paleolaterites in North Karelia, eastern Finland, Geological Society of America Abstracts with Programs, v. 32; 7, p. 486.

Ono, S., and Ohmoto, H., 2000, Constraints on oxygen level of the Archean atmosphere based on new data on dissolution rates of uraninite, Eos, Transactions, American Geophysical Union, v. 81; 48 supplement, p. 1258.

Perry, E.C., and Bonnichsen, B., 1966, Quartz and magnetite: Oxygen 18-Oxygen 16 fractionation in metamorphosed Biwabik formation, Science, v. 153, p. 528-529.

Perry, E.C., Tan, F.C., and Morey, G.B., 1973, Geology and stable isotope chemistry of the Biwabik Iron Formation, northern Minnesota, Economic Geology, v. 68, p. 1110-1125.

Schidlowski, M., 2001, Carbon isotopes as biogeochemical recorders of life over 3.8 Ga of Earth history; evolution of a concept, Precambrian Research, v. 106, 1-2 p. 117-134.

Van Zuilen, M.A., Lepland, A., and Arrehnius, G., 2002, Reassessing the evidence for the earliest traces of life, Nature, v. 418; 6898, p. 627-630.

**Appendix 2.** GPS coordinates for samples of the Upper Cherty member of the Biwabik iron-formation collected in this study.

| | | Location | | | |
|---|---|---|---|---|---|
| Sample # | UW Number | N | | W | |
| 03 BIW 1; A-J | 1962 / 1.1-1.10 | 47° | 39.281 | 91° | 57.202 |
| 03 BIW 2; A-F | 1962 / 2.1-2.6 | 47° | 43.584 | 91° | 50.055 |
| 03 BIW 3; A-E | 1962 / 3.1-3.5 | 47° | 42.365 | 91° | 51.153 |
| 03 BIW 4; A-C | 1962 / 4.1-4.3 | 47° | 43.633 | 91° | 50.028 |
| 03 BIW 5 | 1962 / 5 | 47° | 42.250 | 91° | 51.218 |
| 03 BIW 6; A-E | 1962 / 6.1-6.5 | 47° | 42.233 | 91° | 51.218 |
| 03 BIW 7 | 1962 / 7 | 47° | 42.037 | 91° | 51.346 |
| 03 BIW 8; A-F | 1962 / 8.1-8.6 | 47° | 41.960 | 91° | 51.432 |
| 03 BIW 9; A-B | 1962 / 9.1-9.2 | 47° | 43.500 | 91° | 50.172 |
| 03 BIW 10; A-C | 1962 / 10.1-10.3 | 47° | 43.442 | 91° | 50.191 |
| 03 BIW 11 | 1962 / 11 | 47° | 43.395 | 91° | 50.188 |
| 03 BIW 12; A-E | 1962 / 12.1-12.5 | 47° | 43.067 | 91° | 50.540 |
| 03 BIW 13 | 1962 / 13 | 47° | 42.961 | 91° | 50.671 |
| 03 BIW 14; A-B | 1962 / 14.1-14.2 | 47° | 42.937 | 91° | 50.688 |
| 03 BIW 15; A-B | 1962 / 15.1-15.2 | 47° | 43.200 | 91° | 50.435 |
| 03 BIW 16; A-B | 1962 / 16.1-16.2 | 47° | 43.343 | 91° | 50.248 |
| 03 BIW 17; A-E | 1962 / 17.1-17.5 | 47° | 43.759 | 91° | 49.853 |
| 03 BIW 18; A-E | 1962 / 18.1-18.5 | 47° | 43.885 | 91° | 49.685 |
| 03 BIW 19; A-B | 1962 / 19.1-19.2 | 47° | 43.794 | 91° | 49.801 |
| 03 BIW 20; A-E | 1962 / 20.1-20.5 | 47° | 42.515 | 91° | 50.884 |
| 03 BIW 21; A-C | 1962 / 21.1-21.3 | 47° | 41.186 | 91° | 52.126 |
| 03 BIW 22; A-E | 1962 / 22 | 47° | 41.245 | 91° | 52.187 |
| 03 BIW 23; A-E | 1962 / 23.1-23.5 | 47° | 41.057 | 91° | 52.421 |
| 03 BIW 24; A-E | 1962 / 24.1-24.5 | 47° | 41.010 | 91° | 52.375 |
| 03 BIW 25; A-F | 1962 / 25.1-25.6 | 47° | 41.019 | 91° | 52.363 |
| 03 BIW 26; A-C | 1962 / 26.1-26.3 | 47° | 40.687 | 91° | 52.742 |
| 03 BIW 27; A-D | 1962 / 27.1-27.4 | 47° | 40.812 | 91° | 52.755 |
| 03 BIW 28; A-D | 1962 / 28.1-28.4 | 47° | 40.749 | 91° | 52.908 |
| 03 BIW 30; A-E | 1962 / 30.1-30.5 | 47° | 40.624 | 91° | 53.208 |
| 03 BIW 31; A-E | 1962 / 31.1-31.5 | 47° | 40.268 | 91° | 53.547 |
| 03 BIW 32; A-E | 1962 / 32.1-32.5 | 47° | 40.233 | 91° | 53.882 |
| 03 BIW 33; A-E | 1962 / 33.1-33.5 | 47° | 40.332 | 91° | 53.952 |
| 03 BIW 34; A-E | 1962 / 34.1-34.5 | 47° | 35.755 | 91° | 6.167 |
| 03 BIW 35; A-G | 1962 / 35.1-35.7 | 47° | 35.057 | 91° | 7.463 |
| 03 BIW 36; A-P | 1962 / 36.1-36.16 | 47° | 33.837 | 91° | 9.046 |
| 03 BIW 37; A-D | 1962 / 37.1-37.4 | 47° | 33.527 | 91° | 14.717 |
| 03 BIW 38; A-E | 1962 / 38.1-38.5 | 47° | 35.626 | 91° | 4.843 |
| 03 BIW 39; A-E | 1962 / 39.1-39.5 | 47° | 43.594 | 91° | 49.950 |
| 03 BIW 40; A-C | 1962 / 40.1-40.3 | 47° | 44.009 | 91° | 49.209 |
| 03 BIW 41; A-C | 1962 / 41.1-41.3 | 47° | 43.772 | 91° | 49.718 |
| 03 BIW 42; A-E | 1962 / 42.1-42.5 | 47° | 43.764 | 91° | 49.740 |
| 03 BIW 43; A-E | 1962 / 43.1-43.5 | 47° | 43.806 | 91° | 49.738 |
| 03 BIW 44; A-E | 1962 / 44.1-44.5 | 47° | 39.238 | 91° | 57.483 |
| 03 BIW 45; A-E | 1962 / 45.1-45.5 | 47° | 39.426 | 91° | 57.604 |
| 03 BIW 46; A-E | 1962 / 46.1-46.5 | 47° | 38.195 | 91° | 0.258 |
| 03 BIW 47; A-E | 1962 / 47.1-47.5 | 47° | 35.800 | 91° | 5.935 |
| 03 BIW 48; A-E | 1962 / 48.1-48.5 | 47° | 35.373 | 91° | 5.099 |

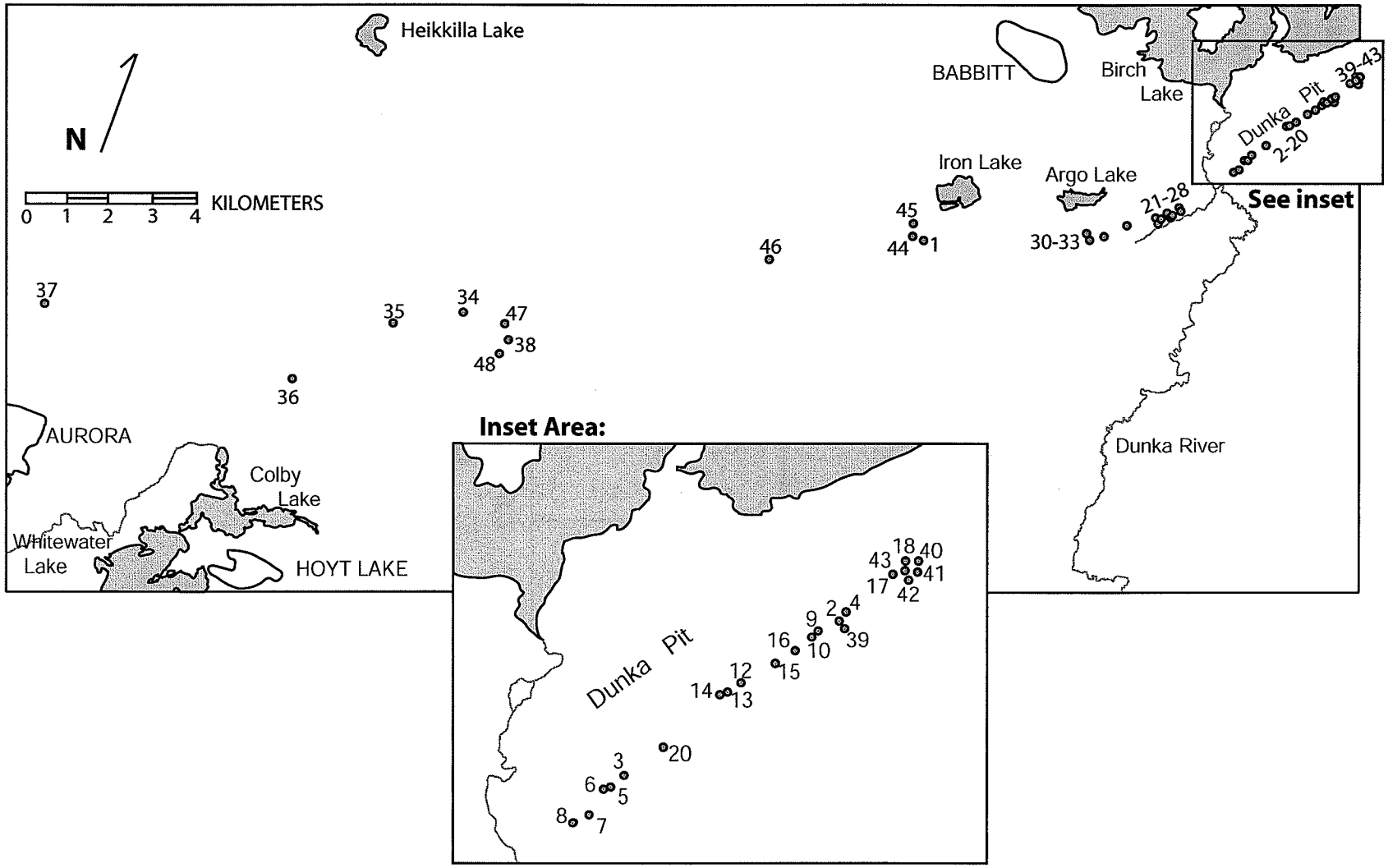


**Appendix 3.** Map of sample locations collected from the Upper Cherty member of the Biwabik iron-formation in this study.

**Appendix 4.** Figure 1. of Jaeger (1959). The ratio of the maximum temperature, $T_m$, attained at distance X from the margin of a sheet of thickness D to the initial contact temperature. Curves 1 to 7 are for various values of the thermal properties and latent heat. Curve 5 was used in this study and has equal thermal properties (thermal conductivity and diffusivity) for the country rock and magma. The range of solidification is 1100- 800 °C and latent heat is 418 J/gm.

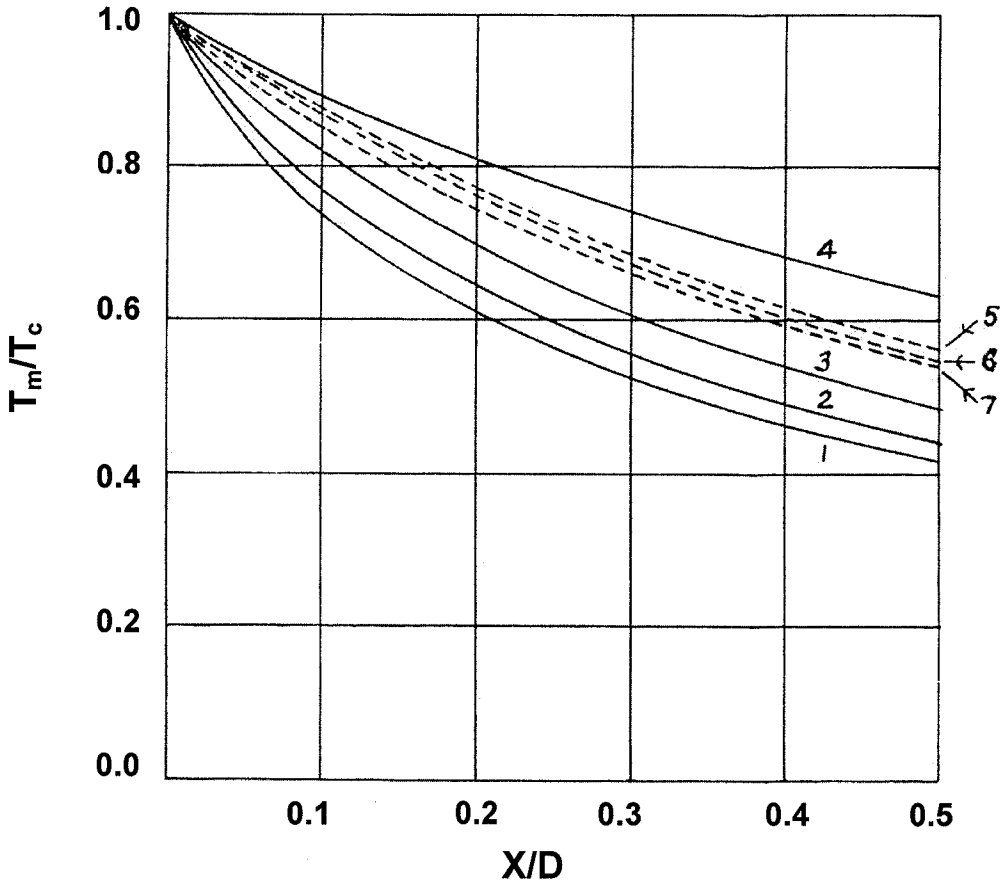

**Appendix 5.** Calibrations of $\Delta^{18}O$ (Qt-water), $\Delta^{18}O$ (silica-water), $\Delta^{18}O$ (Mt-water), and $\Delta^{18}O$ (Qt-Mt).

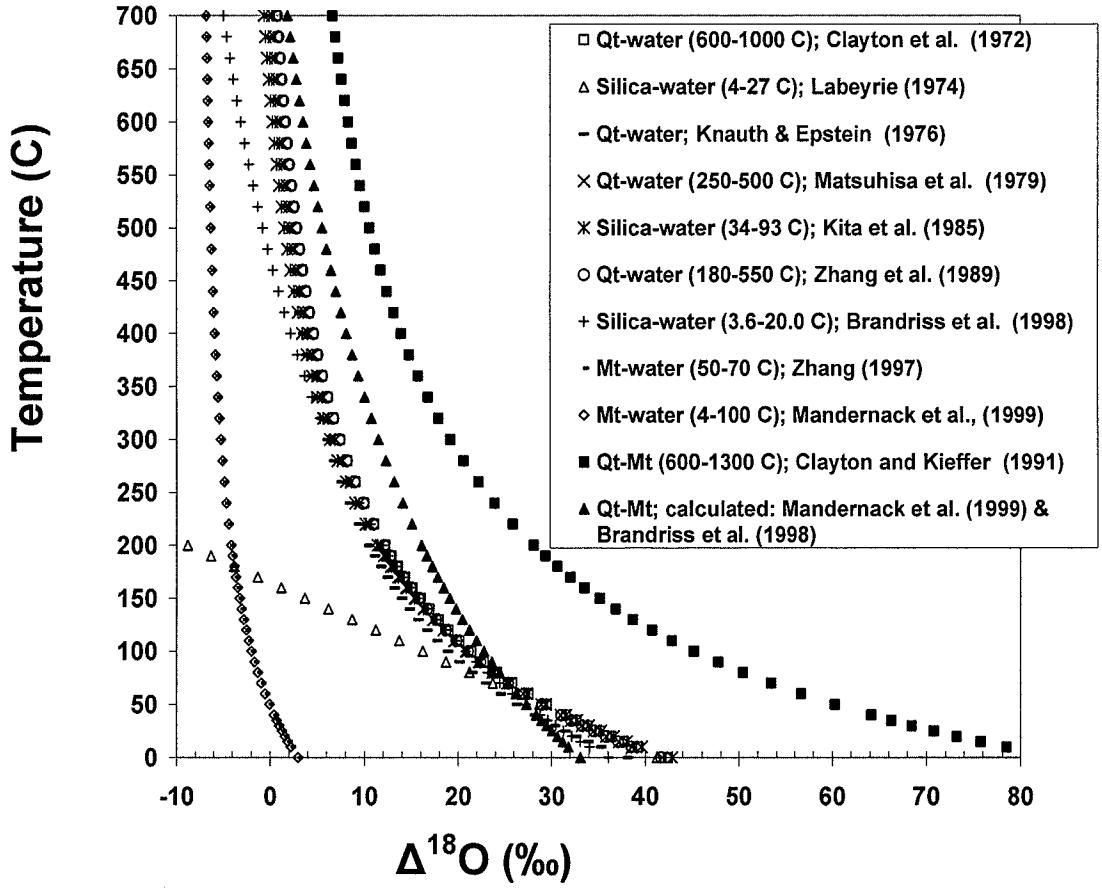

## REFERENCES CITED

Brandriss, M.E., O'Neil, J.R., Edlund, M.B., and Stoermer, E.F., 1998, Oxygen isotope fractionation between diatomaceous silica and water, Geochimica et Cosmochimica Acta, v. 62; 7, p. 1119-1125.

Clayton, R.N., and Kieffer, S.W., 1991, Oxygen isotopic thermometer calibrations, The Geochemical Society Special Publication, v. 3, p. 3-10.

Clayton, R.N., O'Neil, J.R., and Mayeda, T.K., 1972, Oxygen isotope exchange between quartz and water, Journal of Geophysical Research, v. 77, p. 3057-3067.

Kita, J., Taguchi, S., and Matsubaya, O., 1985, Oxygen isotope fractionation between amorphous silica and water at 34-93 °C, Nature, v. 314; 7, p. 83-84.

Knauth, L.P., and Epstein, S., 1976, Hydrogen and oxygen isotope ratios in nodular and bedded cherts, Geochimica et Cosmochimica, v. 40, p. 1095-1108.

Labeyrie, L., 1974, New approach to surface water paleotemperatures using $^{18}O/^{16}O$ ratios in the silica of diatom frustrules, Nature, v. 248, p. 40-41.

Mandernack, K.W., Bazylinski, D.A., Shanks III, W.C., and Bullen, T.D., 1999, Oxygen and iron isotope studies of magnetite produced by magnetotactic bacteria, Science, v. 285, p. 1892-1896.

Matsuhisu, Y., Goldsmith, J.R., and Clayton, R.N., 1979, Oxygen isotopic fractionation in the system quartz-albite-anorthite-water, Geochimica et Cosmochimica Acta, v. 43, p. 1131-1140.

Zhang, C., Lui, J., Chen, Z., and Zhou, H., 1989, Oxygen isotope fractionation in the quartz-water-salt system, Economic Geology, v. 84, p. 1643-1650.

Zhang, C., Liu, S., Phelps, T.J., Cole, D.R., Horita, J., Fortier, S.M., Elless, M., and Valley, J.W., 1997, Physiochemical, mineralogical, and isotopic characterization of magnetite-rich iron oxides formed by thermophilic iron-reducing bacteria, Geochimica et Cosmochimica Acta, v. 61; 21, p. 4621-4632.

APPROVED BY:

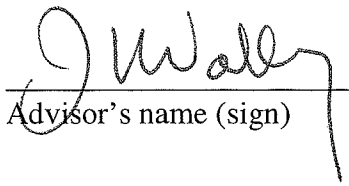

Advisor's name (sign)

John W. Valley

Advisor's name (print)

9-28-04

(Date)